# Novel approach using cell-penetrating peptides for efficient intestinal absorption of therapeutic peptides and proteins

**Noriyasu Kamei**

# CONTENTS

# LIST OF PUBLICATIONS

1. A novel approach using functional peptides for efficient intestinal absorption of insulin. Mariko Morishita, Noriyasu Kamei, Jumpei Ehara, Koichi Isowa, Kozo Takayama. *J. Control. Release* 118 (2007) 177-184. <presented in Chapter 1 of this dissertation>

2. Usefulness of cell-penetrating peptides to improve the intestinal insulin absorption. Noriyasu Kamei, Mariko Morishita, Yoshimi Eda, Nobuo Ida, Reiji Nishio, Kozo Takayama. *J. Control. Release* 132 (2008) 21-25. <presented in Chapter 2 of this dissertation>

3. Permeation characteristics of oligoarginine through intestinal epithelium and its usefulness for intestinal peptide drug delivery. Noriyasu Kamei, Mariko Morishita, Jumpei Ehara, Kozo Takayama. *J. Control. Release* 131 (2008) 94-99. <presented in Chapter 3 of this dissertation>

4. Importance of intermolecular interaction on the improvement of intestinal therapeutic peptide/protein absorption using cell-penetrating peptides. Noriyasu Kamei, Mariko Morishita, Kozo Takayama. *J. Control. Release* (submitted). <presented in Chapter 4 of this dissertation>

# ABBREVIATIONS

| | |
|---|---|
| AAC | area above the blood glucose concentration curve |
| ANOVA | analysis of variance |
| AUC | area under the plasma concentration curve |
| BA | bioavailability |
| $B_{max}$ | maximum binding capacity |
| $C_{max}$ | peak plasma concentration |
| CPP | cell-penetrating peptide |
| ELISA | enzyme-linked immunosorbent assay |
| FD-4 | fluorescein isothiocyanate-labeled dextran 4,400 |
| FL | fluorescein |
| GLP-1 | glucagon-like peptide-1 |
| HIV-1 | human immunodeficiency virus-1 |
| IFN-β | interferon β |
| i.p. | intraperitoneal |
| $I_{sc}$ | short-circuit current |
| i.v. | intravenous |
| $J_{ss}$ | steady-state flux |
| KD | dissociation constant |
| LDH | lactate dehydrogenase |
| PA | pharmacological availability |
| $P_{app}$ | apparent permeability coefficient |
| PBS | phosphate-buffered saline |

| | |
|---|---|
| PD | transmucosal potential difference |
| pI | isoelectric point |
| Rm | membrane electrical resistance |
| $R_{max}$ | maximum binding amount |
| R6 | arginine-hexamer |
| R8 | arginine-octamer |
| R10 | arginine-decamer |
| R12 | arginine-dodecamer |
| s.c. | subcutaneous |
| SPR | surface plasmon resonance |
| $T_{max}$ | time taken to reach the peak plasma concentration |

# GENERAL INTRODUCTION

During the past few decades, advances in molecular biology have brought us a wide variety of peptide- and protein-based pharmaceuticals for treating various diseases [1-3]. The contribution to the treatment of disease by these drugs is significant, and it is thought that clinical development of these drugs will increase in the future. In contrast, at present, these drugs are mainly administered through peripheral routes, such as intravenous (i.v.) and subcutaneous (s.c.) injections, because the properties in the intestinal tract of such biotechnology-based drugs limit their administration routes and formulation designs (Fig. 1) [4-7]. Even insulin, one of the most widely prescribed peptide drugs, has a restricted delivery route by s.c. injections. For instance, the permeation of peptides and proteins administered via the oral route through the lipid bilayer is extremely limited because of their hydrophilicity. Moreover, they cannot permeate through the paracellular route that is the pathway for hydrophilic compounds because of their molecular weights. In addition, orally administered peptides and proteins are immediately degraded through the action of various enzymes such as trypsin and aminopeptidase in the intestinal lumen and cytoplasm. Although such properties of the intestinal epithelium are essential to protect its vital function from exogenous pathogens, these often become a significant disadvantage for the intestinal absorption of peptides and proteins [4-9]. However, patients find the oral forms of therapeutic drugs more attractive than the injectable forms because oral forms are more convenient and easier to use. To yield therapeutic activity, orally administered biotherapeutic agents need to circumvent such enzymatic and permeation barriers of the gastrointestinal tract to achieve sufficient absorption into the systematic circulation.

Resistance of these drugs to enzymatic degradation was improved in part by strategies such as protease or peptidase inhibitors [10-12] and carrier systems such as micro- and nano-sized particles [13,14], liposomes [15-17], emulsions [18,19], and hydrogels [20-22]. However, it is clear that there will be limited success from strategies directed at overcoming the enzymatic barrier alone. Unless one can increase the membrane permeability of therapeutic peptides and proteins, it is unlikely that high oral bioavailability will be achieved [6]. Although there are some permeation enhancers that facilitate the poor permeation of these drugs through the epithelial membrane [10,23,24], advances in these reagents for clinical use are limited by mechanisms including the disturbance of the epithelial lipid membrane and the opening of tight junctions, which lead to the uptake of drugs plus pathogens and toxins into the circulation as the intestinal epithelium functions as an essential barrier to exogenous pathogens. A secure strategy to improve the absorption of these drugs across the intestinal epithelial barrier is essential to achieve sufficient oral bioavailability to enable clinical use.

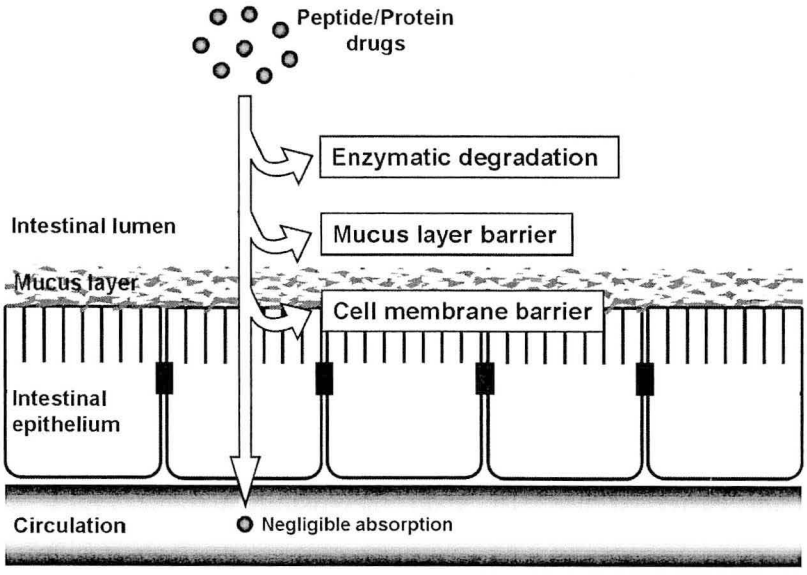


Fig. 1. Inherent barriers to oral absorption of therapeutic peptides and proteins in the gastrointestinal tract. These barriers consist of enzymatic degradation in gastrointestinal lumen and intracellular compartment, mucus layer lying on the microvillus, and lipid bilayer-based cell membrane.

Meanwhile, in recent decades it has been reported that the cell-penetrating peptides (CPPs) including arginine-rich peptides such as human immunodeficiency virus (HIV)-1Tat (48–60) [25-30] and oligoarginine, an oligomer of arginine (one of the basic amino acids) containing six or more amino acids [25-28,30,31] and amphipathic peptides such as penetratin derived from the third helix of the *Drosophila* Antennapedia homeodomain protein [32] (Table 1) can be efficiently introduced into the intracellular space via adsorption to cell-surface proteoglycans and subsequent endocytotic pathway [33-39], especially macropinocytosis [40,41]. Moreover, the conjugation of CPPs with poorly internalized macromolecules such as proteins [42,43] and nucleic acids [44], antibodies [45], and drug-delivery carriers such as liposomes [34,46-48] promotes their introduction into the cytoplasm and nucleus. CPPs can also translocate through the membranes of numerous cells because of their low cell specificity. Therefore, CPPs have frequently been employed as useful tools for intracellular delivery of therapeutic macromolecules. Although there is only limited information about their effects on the membrane permeability of macromolecular drugs, one study reported that insulin transport across Caco-2 cells was dramatically increased by conjugation of insulin with Tat peptide [49]. Therefore, I speculated that peptide and protein drug absorption from the intestine might be improved by using this behavior of CPPs. At present, however, the CPP strategy research lacks sufficient numbers of *in vivo* studies to demonstrate their therapeutic potential. In this study, I applied such ability of CPP to intestinal delivery approach for therapeutic peptides and proteins.

Table 1. Examples of peptide vectors for intracellular delivery [26]

| Peptides | Sequences |
|---|---|
| *Basic peptids* | |
| **HIV-1 Tat (48-60)** | **GRKKRRQRRRPPQ** |
| **Oligoarginine** | **Rn (n=~7-11)** |
| *Basic/amphiphilic peptides* | |
| **Antennapedia (43-58) (penetratin)** | **RQIKIWFQNRRMKWKK** |
| **Model amphipathic peptide** | **KLALKLALKALKAALKLA-amide** |
| *Chimera peptides* | |
| **Transportan (galanin/mastoparan)** | **GWTLNSAGYLLGKINLKALAALAKKIL** |
| **Pep-1 (hydrophobic/NLS)** | **KETWWETWWTEWSQPKKKRKV-cysteamine** |
| *Hydrophobic peptide* | |
| **Membrane translocating sequence peptide** | **AAVALLPAVLLALLP** |

A: Alanine, E: Glutamic acid, F: Phenylalanin, G: Glycine, I: Isoleucine, K: Lysine, L: Leucine, M: Methionine, N: Asparagine, P: Proline, Q: Glutamine, R: Arginine, S: Serine, T: Threonine, V: Valine,W: Tryptophan, Y: Tyrosine.

In Chapter 1, I evaluated whether CPPs can improve intestinal absorption of macromolecular drugs and compounds in rats. As shown in Fig. 2, the coadministration of CPP with macromolecular drug and the administration of CPP-drug conjugate are considered as the strategies using CPP to enhance their intestinal absorption. In this chapter, I evaluated the effect of oligoarginine, typical CPP, on the intestinal absorption of insulin, interferon β (IFN-β) and fluorescein isothiocyanate-labeled dextran 4,400 (FD-4) after coadministration of oligoarginine which is more convenient approach. Furthermore, I examined whether oligoarginine has the unfavorable effect to intestinal mucosal membrane for safe use of oligoarginine. In addition, I evaluated the effect of chain length of oligoarginine on the improvement of intestinal drug absorption by coadministration of oligoarginine. In Chapter 2, to find out the more effective and safer CPP on the improvement of intestinal insulin absorption, I screened the ability of various CPP such as oligoarginine and penetratin to enhance the intestinal insulin

absorption. In Chapters 3 and 4, I examined the mechanisms underlying the improvement of intestinal drug absorption by coadministration of CPP. In Chapter 3, I evaluated the permeation characteristics of oligoarginine through intestinal epithelial membrane. Furthermore, I also evaluated the intestinal absorption of fusogenic leuprolide which is conjugated with oligoarginine to examine the potential of another approach in which conjugate of drug and CPP was used as shown in Fig. 2 (a). In Chapter 4, I clarified the importance of intermolecular interaction between drug and CPP on the improvement of intestinal drug absorption by coadministration of CPP.

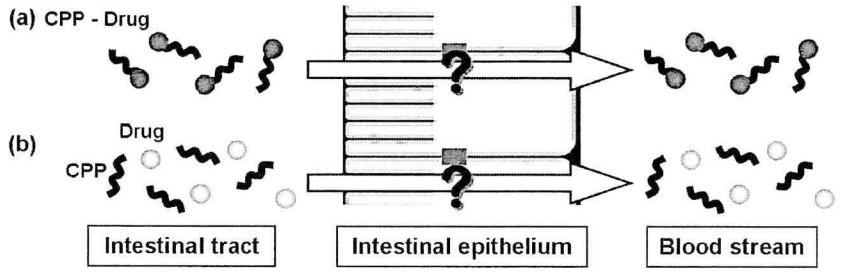


Fig. 2. Schematic illustration of CPP-based intestinal delivery strategy for therapeutic peptides and proteins. (a) Conjugation of peptides/proteins with CPP. (b) Physical mixture of peptides/proteins and CPP.

# Chapter 1

# Novel approach using functional peptides for efficient intestinal absorption of insulin

## 1. Introduction

It is clear that strategies directed at overcoming the enzymatic barrier alone will have only limited success in the development of oral forms of peptide and protein drugs. High oral bioavailability is unlikely to be achieved unless one can increase the membrane permeability of macromolecules. Recent reports using CPPs indicate that drugs that are poorly permeable through the cell membrane can be taken up efficiently by diverse cells without altering drug activity [25-27]. Therefore, I speculated that peptide and protein drug absorption from the intestine might be improved by using this behavior of CPPs.

In this chapter, I evaluated whether CPPs can improve intestinal absorption of insulin in rats. The effect of CPPs on macromolecular intestinal absorption was further examined using IFN-β and FD-4 macromolecules as model macromolecular solutes. Peptides composed of six (R6), eight (R8), and 10 (R10) residues of arginine were used as the CPP. To assess the safety of CPP in the intestinal epithelium, I also measured the leakage of lactate dehydrogenase (LDH), an intracellular enzyme inherent in the enterocyte of the intestinal epithelium, and performed light microscopic observation of intestinal tissues after pretreatment with oligoarginine.

## 2. Materials and methods

### 2.1. Materials

Recombinant human insulin (26 IU/mg), 20% formalin neutral buffer solution, and LDH Test Wako were purchased from Wako Pure Chemical Industries, Ltd. (Osaka, Japan). L-R6 (RRRRRR, R: L-arginine), D-R6 (rrrrrr, r: D-arginine), D-R8 (rrrrrrrr), D-R10 (rrrrrrrrrr), FD-4, and sodium taurodeoxycholate were purchased from Sigma-Aldrich Co. (St. Louis, MO, USA). IFN-β ($0.6 \times 10^7$ IU/vial) was kindly supplied by Toray Industries, Inc. (Kanagawa, Japan). All other chemicals were of analytical grade and commercially available.

### 2.2. Preparation of drug and oligoarginine solution

Specific amounts of recombinant human insulin were dissolved in 50 μL of 0.1 M HCl in polypropylene tubes. The insulin solution was diluted with 2.4 mL of phosphate-buffered saline (PBS, pH 7.4) containing 0.001% methylcellulose, which prevents the adsorption of insulin on the tube surface, and normalized with 50 μL of 0.1 M NaOH. The FD-4 solution was prepared at 2 mg/mL, and the IFN-β solution at $0.9 \times 10^6$ IU/mL, in PBS. Specific amounts of L-R6, D-R6, D-R8, or D-R10 was measured in the polypropylene tubes, and an aliquot of drug solution was added to the tubes and mixed gently to yield a clear solution.

### 2.3. In situ loop absorption study

This research was performed at Hoshi University and complied with the regulations of the Committee on Ethics in the Care and Use of Laboratory Animals. Male Sprague Dawley rats weighing 180–220 g were purchased from Tokyo Laboratory

Animals Science Co., Ltd. (Tokyo, Japan). Animals were housed in rooms controlled between 23 ± 1 °C and 55 ± 5% relative humidity, and they had free access to water and food during acclimatization. Animals were fasted for 24 h before the experiments. Following anesthetization by intraperitoneal (i.p.) injection of sodium pentobarbital (50 mg/kg; Dainippon Sumitomo Pharm Co., Ltd., Osaka, Japan), rats were restrained in a supine position on a thermostatically controlled board at 37 °C. Additional i.p. injections of sodium pentobarbital (12.5 mg/kg) were used every 1 h to maintain the anesthesia.

The ileum was exposed following a small midline incision made carefully in the abdomen, and its proximal-to-ileocecal junction segments (length = 10 cm) were cannulated at both ends using polypropylene tubing. These were ligated securely to prevent fluid loss and returned carefully to their original location inside the peritoneal cavity. To wash the intestinal content, PBS warmed at 37 °C was circulated through the cannula at 5.0 mL/min for 8 min using an infusion pump (KD Scientific Inc., Holliston, MA, USA). The cannulation tubing was removed and the segments were then closed tightly; about 1 mL of perfusion solution remained in the segments. Rats were left on the board at 37 °C for a further 30 min to recover from the elevated blood glucose concentration resulting from the surgery described above. After the 30 min rest, 0.5 mL of drug–oligoarginine mixed solution or drug solution (control) was administered directly into the 6 cm ileal loop made from the 10 cm pretreated segment. The doses were 50 IU/kg body weight for insulin, 5 mg/kg for FD-4, and $2.25 \times 10^6$ IU/kg for IFN-β. For evaluating the effect of L- and D-R6 on insulin intestinal absorption, the doses of oligoarginines were 6.25, 12.5, and 25.0 mg/kg body weight. For evaluating the effect of chain length of oligoarginine on insulin intestinal absorption, the doses of

D-R6, D-R8 and D-R10 were 6.25, 8.3 and 10.35 mg/kg, respectively, and the molar concentration of these administration solutions was the same (2.6 mM).

The relative bioavailability of enterally administered insulin was calculated relative to the s.c. route. Briefly, an insulin solution was prepared by dissolving an appropriate amount of recombinant human insulin in PBS at an s.c. dose of 1.0 IU/kg body weight. To maintain the same physical conditions for the rats, the same surgery (ileal loop) was performed on animals receiving s.c. insulin as on rats in the intestinal absorption study.

During the experiment, a 0.25 mL blood aliquot was taken from the jugular vein before and 5, 10, 15, 30, 60, 120, 180, and 240 min after dosing. Tuberculin syringes (1 mL) were preheparinized in the usual fashion by coating the syringe wall with aspirating heparin and then expelling all heparin by depressing the plunger to the needle hub. Plasma was separated by centrifugation at 13,000 rpm (13,400 × *g*) for 1 min. Blood glucose concentration was measured with a glucose meter (Novo Assist Plus, Novo Nordisk Pharma Ltd., Tokyo, Japan) in the insulin studies and used to represent the biological activity of insulin. The biological activity of insulin is expressed as a percentage of the predose glucose concentration adjusted to the corresponding blood glucose concentration in the control group (insulin solution). The magnitude of the hypoglycemic response was calculated using the trapezoidal method as the area above the curve (AAC) for 0–4 h. The plasma insulin concentration was determined using an enzyme immunoassay (Insulin ICMA kit, Molecular Light Technology, Wales, UK). The total area under the insulin concentration curve (AUC) from 0–4 h was estimated from the sum of successive trapezoids between each data point. The bioavailability was calculated relative to the s.c. injection as described above. The peak plasma concentration ($C_{max}$) and the time taken to reach the peak plasma concentration ($T_{max}$)

were determined from the plasma insulin concentration–time curve. Plasma IFN-β concentration was determined using an enzyme immunoassay (IFN-β ELISA kit, Toray Industries, Inc., Kanagawa, Japan). Plasma FD-4 concentration was determined using a microplate luminometer (Mithras LB940, Berthold Japan, Tokyo, Japan) at excitation and emission wavelengths of 485 and 535 nm, respectively.

### 2.4. LDH leakage

LDH leakage from the intestinal membrane, one of the indices of toxicity assessment, was measured after incubation with CPP for a predetermined time. The 6 cm ileal loop made from the 10 cm pretreated segment, as described above, was used for these experiments. The ileum was treated with 20 mL of PBS warmed to 37 °C and then flushed out with air. A solution of 0.5 mL PBS, 1% (w/v) sodium taurodeoxycholate, L-R6 (25.0 mg/kg), or D-R6 (25.0 mg/kg) was administered to the ileum and left in the ileal segments for 2 h. After the 2 h incubation, the ileal loop was washed with 3 mL PBS and the intestinal fluid was collected. The concentration of LDH in the fluid was determined using the LDH Test Wako (Wako Pure Chemical Industries, Ltd., Osaka, Japan).

### 2.5. Light microscopy

The ileal segments were removed following the 4 h in situ absorption study and fixed with 20% formalin neutral buffer solution. Thin cross-sectional samples were prepared on a microtome and stained with hematoxylin and eosin for light microscopic observation to histologically assess tissue damage.

### 2.6. Statistical analysis

Each value is expressed as the mean ± standard error (S.E.) of 3-8 determinations. For group comparisons, analysis of variance (ANOVA) with a one-way layout was applied. The mean values were evaluated by Student's unpaired $t$ test and $p < 0.05$ was considered significant.

## 3. Results

### 3.1. Effect of oligoarginine on insulin absorption from the ileum

Figures 3 and 4 show the effect of L-R6 and D-R6 on the ileal insulin absorption (A) and resultant hypoglycemic effect (B). No apparent hypoglycemic response was observed following administration of insulin solution, demonstrating no insulin absorption from the ileal segments. In contrast, coadministration of oligoarginine in a dose-dependent manner increased insulin absorption. As shown in Fig. 4, insulin absorption increased more after treatment with D-R6 than after treatment with L-R6, implying that the more metabolically stable oligoarginine induced the bigger insulin absorption from the ileum.

Table 2 summarizes the pharmacokinetic parameters derived from the insulin concentration–time profiles following in situ administration of insulin with oligoarginine to the ileal segments. AUC is derived from the plasma insulin concentration–time profile, and the area AAC is derived from the blood glucose concentration–time profile. The relative bioavailability (BA) and pharmacological availability (PA) were calculated from data obtained in the s.c. injection study. Although negligible absorption was observed with administration of the insulin solution, L-R6 and D-R6 significantly increased $C_{max}$, AAC, AUC, PA, and BA, which are all related to the extent of absorption. Significant linear relationships resulted after plotting AUC ($r = 0.721$, $p < 0.01$) and AAC ($r = 0.619$, $p < 0.01$) of the insulin vs. dose response to L-R6. Similar patterns were observed for AUC ($r = 0.8328$, $p < 0.01$) and AAC ($r = 0.9074$, $p < 0.01$) of the insulin vs. dose response to D-R6.

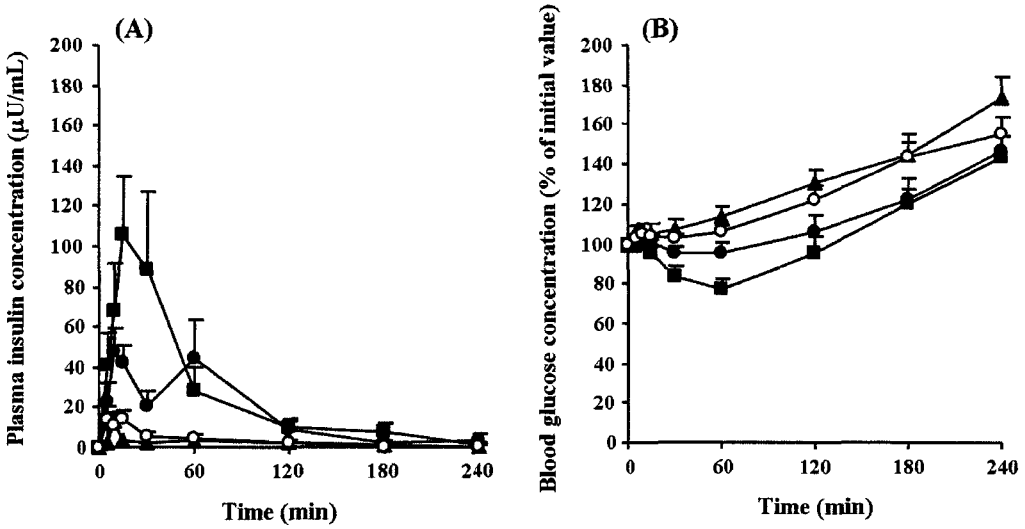


Fig. 3. Plasma insulin (a) and blood glucose (b) concentration vs. time profiles following in situ administration of insulin (50 IU/kg) with various dose of L-R6 into the ileal segments. Each data point represents the mean ± S.E. (n=3–8). Key: (○) insulin-PBS solution (control); (▲) 6.25 mg/kg; (●) 12.5 mg/kg; (■) 25.0 mg/kg of L-R6.

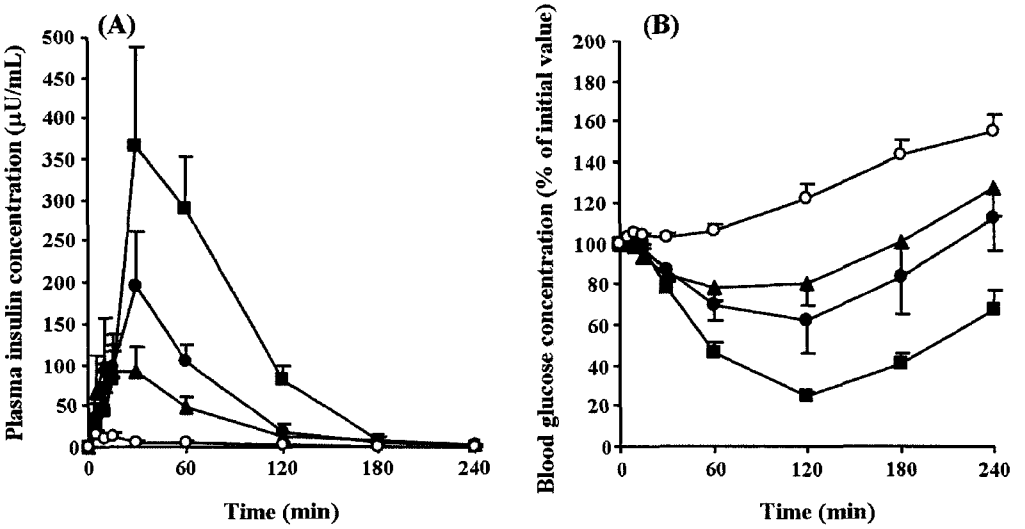


Fig. 4. Plasma insulin (a) and blood glucose (b) concentration vs. time profiles following in situ administration of insulin (50 IU/kg) with various doses of D-R6 into the ileal segments. Each data point represents the mean ± S.E. (n=3–8). Key: (○) insulin PBS solution (control); (▲) 6.25 mg/kg; (●) 12.5 mg/kg; (■) 25.0 mg/kg of D-R6.

Table 2. Pharmacokinetic parameters following in situ administration of insulin with various doses of L- or D-R6 into the ileal segments

| | $C_{max}$ (μU/mL) | $T_{max}$ (min) | AAC (% glu. reduc. ·hr) | AUC (μU·hr/mL) | PA (%) | BA (%) |
|---|---|---|---|---|---|---|
| **Insulin solution** | 16.9 ± 4.6 | 10.0 ± 2.9 | 1.6 ± 0.9 | 12.6 ± 3.5 | 0.1 ± 0.0 | 0.4 ± 0.1 |
| **+ L-R6** | | | | | | |
| **6.25 mg/kg** | 24.0 ± 12.6 | 10.0 ± 2.9 | 0.2 ± 0.2 | 10.1 ± 2.2 | 0.0 ± 0.0 | 0.3 ± 0.1 |
| **12.5 mg/kg** | 64.1 ± 9.1** | 43.3 ± 16.7 | 15.7 ± 10.9 | 65.5 ± 19.1 | 0.7 ± 0.5 | 2.2 ± 0.6 |
| **25.0 mg/kg** | 141.5 ± 27.8* | 25.0 ± 8.2 | 37.9 ± 12.0* | 96.7 ± 22.2* | 1.7 ± 0.5* | 3.3 ± 0.7* |
| **+ D-R6** | | | | | | |
| **6.25 mg/kg** | 116.1 ± 52.3 | 20.0 ± 5.8 | 54.5 ± 18.2 | 120.9 ± 42.4 | 2.4 ± 0.8 | 4.1 ± 1.4 |
| **12.5 mg/kg** | 208.4 ± 62.3 | 33.8 ± 9.4 | 94.8 ± 37.7 | 198.8 ± 27.8** | 4.2 ± 1.7 | 6.7 ± 0.9** |
| **25.0 mg/kg** | 395.6 ± 104.8* | 37.5 ± 7.5* | 214.7 ± 20.4** | 464.0 ± 109.1* | 9.5 ± 0.9** | 15.7 ± 3.7* |

Data: mean ± S.E. (n=3–8).
$C_{max}$, the maximum concentration; $T_{max}$, the time to reach the $C_{max}$; AAC, the area above the curve; AUC, the area under the curve; PA, pharmacological availability compared with s.c.; BA, relative bioavailability compared with s.c.
*$p$<0.05, **$p$<0.01, significant difference compared with the corresponding "insulin solution".

### 3.2. Effect of oligoarginine on IFN-β and FD-4 absorption from the ileum

Table 3 shows the effect of oligoarginine on the intestinal absorption of the protein drug, IFN-β. Although the same dose of L-R6 (25.0 mg/kg) significantly increased the ileal absorption of insulin (Fig. 3 and Table 2), the ileal absorption of IFN-β did not increase in the presence of L-R6. Similarly, neither L-R6 nor D-R6 (25.0 mg/kg) increased the ileal absorption of FD-4, which is representative of hydrophilic macromolecules (Table 4).

Table 3. Pharmacokinetic parameters following in situ administration of IFN-β with L-R6 into the ileal segments

| | $C_{max}$ (IU/mL) | $T_{max}$ (min) | AUC (IU·hr/mL) |
|---|---|---|---|
| **IFN-β solution** | **10.0 ± 4.1** | **103.8 ± 53.8** | **39.2 ± 17.1** |
| **IFN-β + L-R6** | **6.4 ± 1.2** | **50.0 ± 10.0** | **11.9 ± 3.8** |

Dose of L-R6: 25.0 mg/kg.
Data: mean ± S.E. (n=3–6).
$C_{max}$, the maximum concentration; $T_{max}$, the time to reach the $C_{max}$; AUC, the area under the curve.

Table 4. Pharmacokinetic parameters following in situ administration of FD-4 with L- or D-R6 into the ileal segments

| | $C_{max}$ (μg/mL) | $T_{max}$ (min) | AUC (μg·hr/mL) |
|---|---|---|---|
| **FD-4 solution** | **0.3 ± 0.1** | **105.0 ± 90.0** | **0.8 ± 0.9** |
| **FD-4 + L-R6** | **0.6 ± 0.2** | **40.0 ± 17.3** | **1.2 ± 1.1** |
| **FD-4 + D-R6** | **0.7 ± 0.2** | **120.0 ± 60.0** | **2.0 ± 1.1** |

Dose of L- or D-R6: 25.0 mg/kg.
Data: mean ± S.E. (n=3–4).
$C_{max}$, the maximum concentration; $T_{max}$, the time to reach the $C_{max}$; AUC, the area under the curve.

### 3.3. Effect of chain length of oligoarginine on insulin absorption from the ileum

Insulin was coadministered with oligoarginine composed of six, eight, or 10 arginine residues (6.25, 8.3 or 10.35 mg/kg, respectively) to the ileum, and their effects on insulin absorption were compared (Fig. 5). As shown in Fig. 5, D-R8 and D-R10 enhanced insulin absorption from the intestine more markedly than did D-R6. Table 5 summarizes the pharmacokinetic parameters derived from the insulin concentration–time profiles shown in Fig. 5. D-R8 caused the greatest increase in

intestinal insulin absorption. Compared with D-R6, D-R8 had 3.4-times higher relative BA and D-R10 had 2.7-times higher relative BA for insulin.

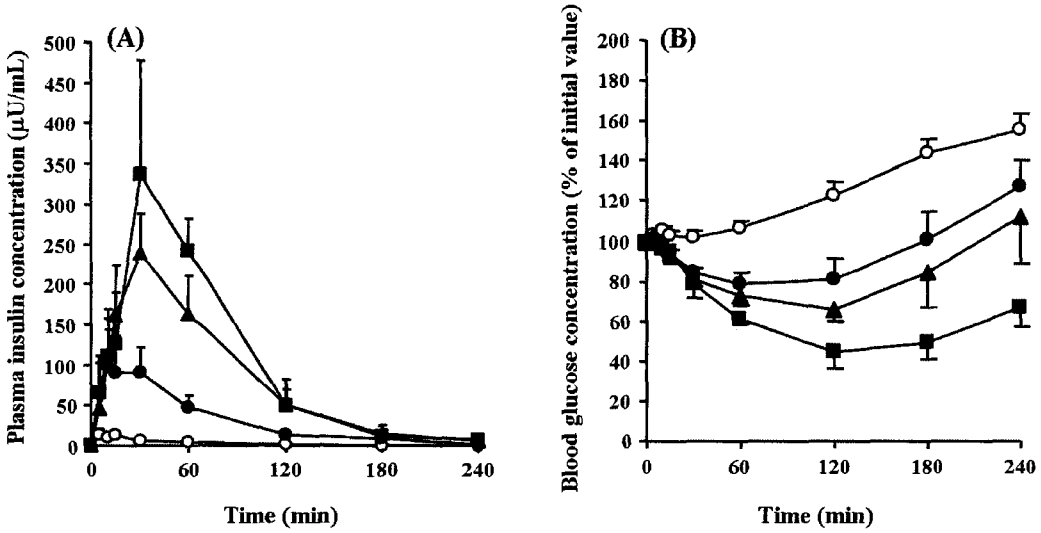


Fig. 5. Plasma insulin (a) and blood glucose (b) concentration vs. time profiles following in situ administration of insulin (50 IU/kg) with D-R6 (6.25 mg/kg), D-R8 (8.3 mg/kg) or D-R10 (10.35 mg/kg) into the ileal segments. Each data point represents the mean ± S.E. (n=3-8). Key: (○) insulin PBS solution (control); (●)D-R6; (■)D-R8; (▲)D-R10.

Table 5. Pharmacokinetic parameters following in situ administration of insulin with D-R6, D-R8, and D-R10 into the ileal segments

| | $C_{max}$ (μU/mL) | $T_{max}$ (min) | AAC (% glu. reduc. · hr) | AUC (μU · hr/mL) | PA (%) | BA (%) |
|---|---|---|---|---|---|---|
| **Insulin solution** | 16.9 ± 4.6 | 10.0 ± 2.9 | 1.6 ± 0.1 | 12.6 ± 3.5 | 0.1 ± 0.0 | 0.4 ± 0.1 |
| **+ D-R6** | 116.1 ± 52.3 | 20.0 ± 5.8 | 54.5 ± 18.2 | 120.9 ± 42.4 | 2.4 ± 0.8 | 4.1 ± 1.4 |
| **+ D-R8** | 384.0 ± 115.9 | 45.0 ± 8.7* | 222.8 ± 43.8* | 417.7 ± 122.1* | 9.9 ± 1.9* | 14.1 ± 4.1* |
| **+ D-R10** | 238.4 ± 49.3* | 30.0 ± 0.0 | 99.7 ± 41.8 | 322.9 ± 106.9 | 4.4 ± 1.9 | 10.9 ± 3.6 |

Doses of D-R6, D-R8, and D-R10: 6.25, 8.3 and 10.35 mg/kg, respectively, and the molar concentration of these administration solutions was the same (2.6 mM).
Data: mean ± S.E. (n=3–8).
$C_{max}$, the maximum concentration; $T_{max}$, the time to reach the $C_{max}$; AAC, the area above the curve; AUC, the area under the curve; PA, pharmacological availability compared with s.c.; BA, relative bioavailability compared with s.c.
*$p<0.05$, significant difference compared with the corresponding "insulin solution".

### 3.4. Biochemical and histological examinations of the ileal membranes following oligoarginine administration

Table 6 shows data on LDH leakage in the absence (PBS, control) or presence of L- or D-R6 (25.0 mg/kg) in the ileal loop for 2 h. LDH leaked negligibly into the mucosal side, and the LDH leakage was similar in the oligoarginine-treated segments and the PBS-treated segments. In contrast, sodium taurodeoxycholate significantly increased LDH leakage (4.26 vs. 1.19 U).

Figure 6 shows light micrographs of the ileal mucosal membranes pretreated with (a) PBS, (b) L-R6 12.5 mg/kg, (c) L-R6 25.0 mg/kg, and (d) L-R6 37.5 mg/kg for 4 h. The micrographs (Fig. 6) show no apparent histological damage in the L-R6 -treated mucosal membranes compared with the PBS-treated (control) membranes. These data suggest that oligoarginine administration did not alter the ileal membrane integrity.

Table 6. Lactate dehydrogenase (LDH) leakage following PBS (control), L-R6 (25.0mg/kg), D-R6 (25.0 mg/kg) or 1 w/v% sodium taurodeoxycholate pretreatment for 2 h

| Preparation | LDH leakage (U) |
|---|---|
| **Control** | **1.19 ± 0.08** |
| **L-R6** | **1.49 ± 0.11** |
| **D-R6** | **1.55 ± 0.16** |
| **Sodium taurodeoxycholate** | **4.26 ± 0.89 *** |

Data: mean ± S.E. (n=3–5).
*$p<0.05$ compared with control.

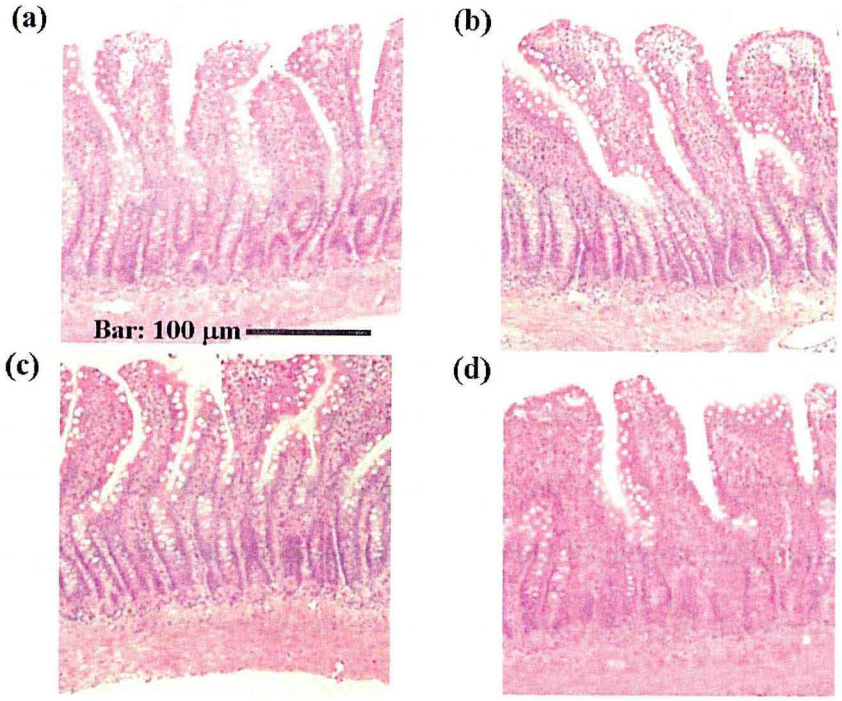


Fig. 6. Light micrographs of the ileal mucosal membranes following in situ administration of (a) insulin–PBS solution, and (b) 12.5 mg/kg, (c) 25.0 mg/kg, and (d) 37.5 mg/kg of L-R6 with insulin for 4 h. The bar indicates 100 μm. Tissues were stained with hematoxylin and eosin following fixation in 20% formalin neutral buffer solution.

## 4. Discussion

In the past decade, studies have indicated that CPPs enable the delivery of different bioactive compounds and drug carriers by chemically hybridizing with target materials [34,42,45,46]. The CPPs deliver their cargo into the cytoplasm by directly perturbing the lipid bilayer structure of the cell membrane or by endocytosis [50,51]. CPPs appear to have little or no toxic effects because penetration causes little disturbance to membranes, and Tat appears to cause practically no harm to cell membranes [51,52]. Toxicity and undesirable side effects have not been detected in most in vivo applications of CPPs [42,51]. These methods are expected to become powerful tools for overcoming the low permeability of peptide and protein drugs through the epithelial cell membrane, which is the greatest barrier to oral delivery of macromolecular drugs. Although structural modification strategies using CPP may be useful, care must be taken not to reduce the biological activity of these drugs. So far, there is little information about whether intermolecular chemical conjugation is essential for a CPP's ability to induce cells to take up macromolecules.

To address these issues, I examined whether oligoarginine enhances the absorption of intestinal bioactive macromolecular drugs without covalently binding to these molecules. As shown in Fig. 3 and Table 2, L-R6 significantly enhanced intestinal insulin absorption and induced a strong hypoglycemic effect in a dose-dependent manner. More pronounced insulin absorption-enhancing effects were observed after D-R6 coadministration with insulin (Fig. 4 and Table 2). To my knowledge, this is the first demonstration that insulin intestinal absorption can be enhanced by a physical mixture containing oligoarginines, and in particular, the D-form. Such mixture preparations are more feasible for delivering protein and peptide drugs than conjugated

forms because they are unlikely to decrease the biological activity of the drug and because they are easy to prepare. These CPP strategies are considered highly promising for the development of an oral delivery system for insulin. In contrast, as shown in Table 3, L-R6 had no enhancing effect on intestinal IFN-β absorption at a dose of 25.0 mg/kg, which was sufficient to increase intestinal absorption of insulin. These results suggest that the ability of oligoarginine to increase intestinal absorption might differ between peptide and protein drugs (molecular weight of insulin: ca. 5.8 kDa and IFN-β: ca. 23 kDa). Further study is needed using various macromolecules of different molecular size and charge to clarify the usefulness of CPPs as oral carriers for bioactive macromolecules.

The L- and D-oligomers of arginine have a similar ability to enter into cells [31]. However, I found that the ability of L- and D-oligomers of arginine to increase absorption differed dramatically in the small intestine. The reason for this difference could be explained by the observation that peptides containing the L-form of amino acids are metabolically more unstable than those containing the D-form [53]. Thus, L-R6 may be degraded rapidly by peptidases that are highly active in the intestinal lumen.

The number of arginines within a peptide sequence has an important influence on the ability of that peptide to enter cells [27,31]. Futaki et al. [27] suggested that R6 and R8 are internalized best by mouse macrophage RAW264.7 cells of peptides composed of 4–16 residues of arginine. Incubation of Jurkat cells, a human T-cell line, with R15 resulted in more intensive internalization than other oligoarginines used [31]. Thus, one may speculate that the extension of an arginine oligomer does not by itself increase the degree of cellular uptake. I used in situ absorption experiments to evaluate the effect of the length of oligoarginine on insulin absorption. The efficiency of enhancement of

bioavailability differed markedly between D-R6, D-R8, and D-R10; D-R8 enhanced insulin mucosal absorption the most efficiently. These results suggest that there is an optimum number of arginines for enhancing intestinal absorption of insulin (Fig. 5 and Table 5). Although the reason why there is an optimal number of arginine residues remains unknown, chain length is presumably associated with the degree of hydrogen bonding with phospholipids, interactions with the cell surface proteoglycans, or permeability of oligoarginine through the mucous layer. A more mechanistic study of the translocation of oligoarginine through cell membranes is required.

I found that the diffusive absorption of macromolecular dextran, FD-4, was not enhanced by coadministration with L- or D-R6 at a concentration (25.0 mg/kg) sufficient to increase insulin absorption (Table 2). Because FD-4 is a hydrophilic compound and a marker of the paracellular pathway, these results exclude the possibility of involvement of opening the paracellular pathway on the insulin absorption-enhancing effect of oligoarginine. In addition, the microscopic observations together with the data on LDH leakage show that the membrane integrity appears to remain undamaged (Fig. 6 and Table 6). These data strongly suggest that the effect of oligoarginines on insulin absorption were not caused by cellular damage.

CPPs are thought to be taken up mainly by cell-mediated macropinocytosis [40,41] through the interaction between the positive charge derived from arginine residues and the negative charge derived from proteoglycans on the cell surface [33-37]. Therefore, I hypothesized that this proposed mechanism could explain how the molecular complex of the drug and oligoarginine is introduced into epithelial cells. I found that oligoarginine enhanced the intestinal absorption of insulin but did not enhance the absorption of other macromolecules such as IFN-β and FD-4. Insulin has a negative

charge in neutral conditions, and insulin may associate with oligoarginine electrostatically. If so, these molecular complexes could be taken up by the interaction between oligoarginine and the surface of epithelial cells. In contrast, IFN-β has a relatively positive charge in neutral conditions, which may set up a repulsive force or prevent intermolecular interaction with oligoarginine. Similarly, noncharged macromolecules, such as FD-4, may not interact with positively charged oligoarginine. A more complete understanding of the mechanisms involved in the CPP-induced enhancement of insulin absorption through the intestinal membrane is needed.

## 5. Conclusions

I have demonstrated that intestinal insulin absorption is enhanced markedly without causing detectable damage in cellular integrity by coadministration of insulin with oligoarginine, but absorption of IFN-β and FD-4 was not enhanced by oligoarginine. The increase in absorption by oligoarginine occurred without chemical hybridization between oligoarginine and insulin. The detailed mechanism responsible for the ability of oligoarginine to increase insulin absorption remains unclear. To develop a macromolecular oral delivery system using oligoarginine, more data on its efficacy and safety and the underlying mechanism are needed.

# Chapter 2

# Usefulness of various cell-penetrating peptides to improve intestinal insulin absorption

## 1. Introduction

In the last chapter, I have demonstrated that oligoarginine known as CPP exerts a significant enhancing effect on intestinal insulin absorption without any untoward effects on the intestinal mucosa. CPPs are peptides that have characteristics that enable them to be readily taken up by several types of cells as well as the ability to bring various substances into the cytoplasm via intermolecular conjugation [34,42-48]. However, I found that an increase in intestinal insulin absorption by oligoarginine occurred without covalent binding between oligoarginine and insulin. This approach has the advantage of not requiring the complicated molecular structure modification process for chemical conjugation and thus the loss of biological activity of peptides and proteins through conjugation.

Oligoarginine could significantly improve the intestinal absorption of insulin; however, this requires relatively high doses of the CPP. Such a high dose of R6 does not show any untoward effects on the intestinal mucosa following administration of a single dose. However, the safety risks involved in the administration of multiple doses and the product cost in actual clinical development mean that safer and more effective CPPs are required to improve the intestinal absorption of various therapeutic peptides and proteins. Therefore, the present study aimed to identify such a CPP for improving the intestinal absorption of biodrugs. Ten different CPPs were selected based on a literature search (Table 7), and their ability to enhance the intestinal bioavailability of insulin was evaluated by the in situ ileal absorption method in rats. In addition, because the absorption enhancing ability of the CPPs depends on the stereoisomeric difference of the peptides as shown in Chapter 1, the effects of the L- and D-forms of CPPs on ileal insulin absorption were compared.

Table 7. Amino acid sequences of cell-penetrating peptides used in this study

| Peptides | Sequence |
|---|---|
| *Arginine rich peptides* | |
| **Arginine octamer (R8)** | **RRRRRRRR** |
| **Arginine dodecamer (R12)** | **RRRRRRRRRRRR** |
| **HIV-1 Tat (48-60)** | **GRKKRRQRRRPPQ** |
| **HIV-1 Rev (34-50)** | **TRQARRNRRRRWRERQR** |
| *Amphipathic peptides* | |
| **Penetratin** | **RQIKIWFQNRRMKWKK** |
| **pVEC** | **LLIILRRRIRKQAHAHSK** |
| **Erns** | **RQGAARVTSWLGLQLRIGK** |
| **RRL helix** | **RRLRRLLRRLRRLLRRLR** |
| **PRL4** | **PRLPRLPRLPRL** |
| *Random composition peptides* | |
| **Random peptide** | **GLSASPNLQFRTV** |

A: Alanine, E: Glutamic acid, F: Phenylalanin, G: Glycine, H: Histidine, I: Isoleucine, K: Lysine, L: Leucine, M: Methionine, N: Asparagine, P: Proline, Q: Glutamine, R: Arginine, S: Serine, T: Threonine, V: Valine,W: Tryptophan.

## 2. Materials and methods

### 2.1. Materials

Recombinant human insulin (26 IU/mg) was purchased from Wako Pure Chemical Industries, Ltd. (Osaka, Japan). L-R8, D-R8, L-R12, HIV-1 Tat (48–60), HIV-1 Rev (34–50), L-penetratin, D-penetratin, L-pVEC, D-pVEC, L-Erns, L-RRL helix, D-RRL helix, L-PRL4, and a random peptide (purity > 95% for each peptide) were purchased from Sigma-Aldrich Co. (St. Louis, MO, USA). All other chemicals were of analytical grade and commercially available.

### 2.2. Preparation of insulin and CPP solution

Specific amounts of recombinant human insulin were dissolved in 50 μL of 0.1 M HCl in polypropylene tubes. The insulin solution was diluted with 2.4 mL of phosphate buffered saline (PBS, pH7.4) containing 0.001% methylcellulose, which prevents the adsorption of insulin on the tube surface, and normalized with 50 μL of 0.1 M NaOH. Specific amounts of CPPs were measured in the propylene tubes, and an aliquot of insulin solution was added to the tubes and mixed gently.

### 2.3. In situ loop absorption study

This research was performed at Hoshi University and complied with the regulations of the Committee on Ethics in the Care and Use of Laboratory Animals, and was performed in the similar procedures as described in Chapter 1. After the surgical process, 0.5 mL of insulin–CPP solution or insulin solution (control) was administered directly into the 6 cm ileal loop made from the 10 cm pretreated segment. The dose of insulin was fixed at 50 IU/kg body weight (132 μM) for all absorption experiments. In

the experiments for comparing the absorption enhancement ability of the CPPs, the dose of each CPP was 1.25 μmol/kg (0.5 mM). In dose-dependent experiments with L- and D-penetratin, the dose was changed to 0.125–5 μmol/kg (0.05–2 mM).

During experiments, a 0.25 mL blood aliquot was taken from the jugular vein before and 5, 10, 15, 30, 60, 120, 180, and 240 min after dosing. Tuberculin syringes (1 mL) were preheparinized in the usual fashion by coating the syringe wall with aspirating heparin and then expelling all heparin by depressing the plunger to the needle hub. Plasma was separated by centrifugation at 13,000 rpm (13,400 × *g*) for 1 min. The plasma insulin concentration was determined using an enzyme immunoassay (Insulin ICMA kit; Molecular Light Technology, Wales, UK). The AUC from 0–4 h, bioavailability relative to the s.c. injection Cmax and Tmax were estimated in the same procedures as described in Chapter 1.

### 2.4. LDH leakage

This examination was performed in the same procedures as described in Chapter 1. After the surgery, a solution of 0.5 mL PBS, 5% (w/v) sodium taurodeoxycholate, and L- or D-penetratin (0.5 mM) was administered to the ileum and left in the ileal segments for 2 h. After the 2 h incubation, the ileal loop was washed with 3 mL PBS and the intestinal fluid was collected. The concentration of LDH in the fluid was determined using the LDH Test Wako (Wako Pure Chemical Industries, Ltd., Osaka, Japan).

### 2.5. Preparation of the intestinal enzymatic fluid

Male Wistar rats (200 g) were purchased from Sankyo Lab Service Co., Ltd. (Tokyo, Japan). Animals were housed in rooms controlled between 23 ± 1 °C and 55 ±

5% relative humidity, and were allowed free access to water and food during acclimatization. The rats were fasted for 24 h and anesthetized by i.p. injection of 50 mg/kg sodium pentobarbital. The rats were secured to the operating table in a supine position and a midline abdominal incision was performed. To obtain the intestinal fluid, a sonde needle was inserted into the upper portion of the small intestine, and the intestine was cannulated on the lower side (length = 20 cm) to remove the intestinal fluid. The contents of the small intestinal were washed out with 30 mL of PBS. This efflux was treated with two volumes of methylene chloride to remove lipid contents, which were contained in the intestinal fluid [54]. The purification was repeated five times. The total protein concentration of the purified intestinal fluid was determined by the method of Lowry. The hydrolytic activity of intestinal enzyme fluid was determined by measuring the degree of insulin degradation using HPLC as described previously [55].

### 2.6. Statistical analysis

Each value is expressed as the mean ± standard error (S.E.) of 3-6 determinations. For group comparisons, analysis of variance (ANOVA) with a one-way layout was applied. The mean values were evaluated by Student's unpaired $t$ test and $p < 0.05$ was considered significant.

## 3. Results

### 3.1. Effect of CPPs on insulin absorption from the ileum

No apparent absorption was observed following administration of the insulin solution in the absence of CPP. Similarly, no apparent insulin absorption was observed when it was coadministered with seven of the 10 CPPs. These were the L-forms of R8, R12, HIV-Rev, HIV-Tat, Erns, PRL4, and the random peptide (data not shown). In contrast, the L-forms of penetratin, pVEC, and RRL helix significantly increased intestinal insulin absorption. Therefore, I chose these CPPs for further evaluation in terms of stereoisomeric difference. Figure 7 shows the effect of these three selected CPPs on ileal insulin absorption. In this evaluation, R8 was included because I found that D-R8 was a strong bioavailability enhancer for insulin and that the effects on insulin absorption were more pronounced for D-R8 than for D-R6 and D-R10. When the L- or D-form of R8 was coadministered with insulin into the ileal loop, D-R8 markedly enhanced insulin absorption through the ileal membrane compared with L-R8. These results are consistent with the results shown in Chapter 1 using R6 as an effective CPP. In contrast, penetratin, pVEC, and RRL helix showed more significant enhancement of insulin absorption when coadministered in their L-form (0.5 mM).

Table 8 summarizes the pharmacokinetic parameters derived from insulin concentration–time profiles following in situ loop administration of insulin with various CPPs to the ileal segments. The AUC was derived from the plasma insulin concentration–time profiles, and relative bioavailability was calculated from data obtained in the s.c. injection study. Although administration of insulin solution produced negligible absorption, D-R8, L-penetratin, L-pVEC, and L-RRL helix quickly enhanced insulin intestinal absorption and markedly increased the Cmax, AUC, and bioavailability,

which are all related to the extent of insulin absorption. L-penetratin showed the most significant enhancement effects for ileal insulin absorption among the CPPs used in this study. Therefore, L-penetratin was used in further investigations regarding toxicity to the intestinal mucosa and dose-dependent enhancement of insulin absorption.

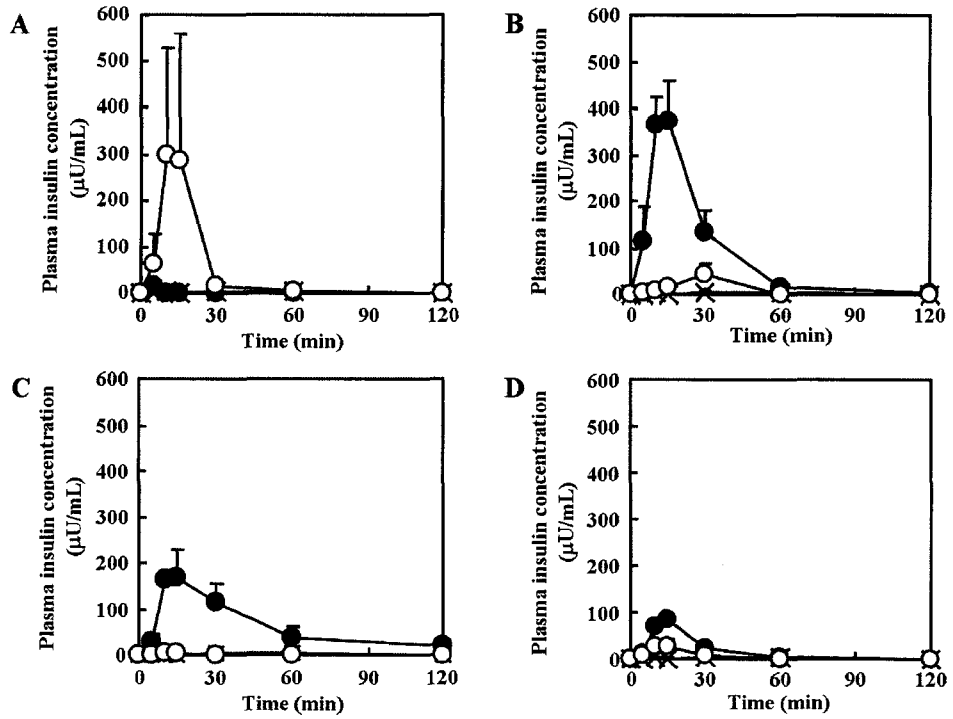


Fig. 7. Plasma insulin concentration vs. time profiles following in situ administration of insulin (50 IU/kg) with 0.5 mM of CPPs into ileal segments. Each data point represents the mean ± S.E. (n=3–6). A: R8, B: Penetratin, C: pVEC, D: RRL helix. Key: (×) insulin–PBS solution; (●) L-peptide; (○) D-peptide.

Table 8. Pharmacokinetic parameters following in situ administration of insulin (50 IU/kg) with CPPs (0.5 mM) into the ileal segments

| | Cmax (μU/mL) | Tmax (min) | AUC (μU·h/mL) | Bioavailability (%) |
|---|---|---|---|---|
| **Insulin solution** | 4.9 ± 1.8 | 76.3 ± 54.9 | 5.7 ± 2.0 | 0.2 ± 0.1 |
| **+ L-R8** | 15.9 ± 13.8 | 46.7 ± 36.8 | 4.1 ± 0.3 | 0.1 ± 0.0 |
| **+ D-R8** | 537.4 ± 261.0 | 18.3 ± 6.0 | 88.1 ± 49.4 | 3.0 ± 1.7 |
| **+ L-Penetratin** | 465.6 ± 50.8** | 13.3 ± 1.1 | 163.8 ± 27.2** | 5.5 ± 0.9** |
| **+ D-Penetratin** | 44.5 ± 20.2 | 23.3 ± 6.7 | 21.2 ± 9.6 | 0.7 ± 0.3 |
| **+ L-pVEC** | 210.4 ± 60.7* | 11.3 ± 1.3 | 121.4 ± 44.7 | 4.1 ± 1.5 |
| **+ D-pVEC** | 5.1 ± 2.5 | 13.3 ± 1.7 | 2.1 ± 0.4 | 0.1 ± 0.0 |
| **+ L-RRL helix** | 84.7 ± 4.2** | 15.0 ± 0.0 | 33.1 ± 4.6** | 1.1 ± 0.2** |
| **+ D-RRL helix** | 32.2 ± 14.7 | 13.3 ± 1.7 | 12.1 ± 5.3 | 0.4 ± 0.2 |

Data: mean ± S.E. (n=3–6).
Cmax: the maximum concentration; Tmax: the time to reach the Cmax; AUC: the area under the curve.
*$p$<0.05, **$p$<0.01: Significant difference to corresponding "Insulin solution".

## 3.2. Biochemical examinations of the ileal membranes following penetratin administration

Table 9 shows the results of LDH leakage in the presence of PBS, L-penetratin or D-penetratin (0.5 mM) in the ileal loop for 2 h. As shown in Table 9, LDH leakage into the intestinal lumen after administration of L- or D-penetratin was negligible and similar to the PBS-treated segments. In contrast, sodium taurodeoxycholate, the positive control, significantly increased LDH leakage.

Table 9. Lactate dehydrogenase (LDH) leakage following PBS, L- and D-penetration (0.5 mM) or 5 w/v% sodium taurodeoxycholate

| | LDH leakage (U) |
|---|---|
| **PBS** | **1.19 ± 0.08** |
| **L-Penetratin** | **2.97 ± 0.62** |
| **D-Penetratin** | **2.16 ± 0.29** |
| **Sodium taurodeoxycholate** | **15.54 ± 2.07*** |

Data: mean ± S.E. (n= 3–5).
*$p<0.05$ against control

### 3.3. Dose-dependent effects of penetratin on ileal insulin absorption

Figure 8 shows ileal insulin absorption following the in situ administration of insulin with various concentrations of L- or D-penetratin, and Table 10 summarizes the pharmacokinetic parameters derived from the insulin concentration–time profiles. The physical mixture of insulin and penetratin formed aggregates and precipitated at a concentration of more than 0.2 mM penetratin. However, L-penetratin enhanced ileal insulin absorption in a dose-dependent manner, even in solutions in which precipitation occurred upon reaching the threshold concentration (over 0.5 mM L-penetratin). A significant linear relationship was observed for the AUC of the insulin vs. dose response to L-penetratin ($r = 0.784$, $p < 0.001$). The relative bioavailability achieved was 35.4% by addition of 2 mM L-penetratin to the insulin solution. In contrast, although D-penetratin also increased ileal insulin absorption in a dose-dependent manner at less than 0.5 mM D-penetratin, this enhancement was diminished in the solution in which

precipitation occurred upon reaching the threshold concentration (over 0.5 mM D-penetratin).

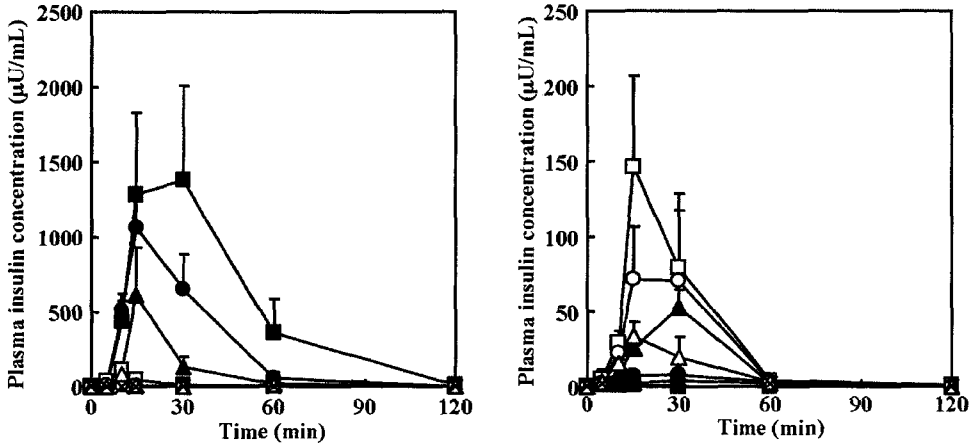


Fig. 8. Plasma insulin concentration vs. time profiles following in situ administration of insulin (50 IU/kg)with various concentrations of L- or D-penetratin into ileal segments. Each data point represents the mean ± S.E. (n=3 or 4). Left: L-penetratin, Right: D-penetratin. Key: (×) insulin-PBS solution; (Δ) 0.05mM; (○) 0.1mM; (□) 0.2mM; (▲) 0.5mM; (●) 1mM; (■) 2 mM of penetratin.

Table 10. Pharmacokinetic parameters following in situ administration of insulin (50 IU/kg) with various concentrations of L- or D-penetratin into the ileal segments

| | Cmax (uU/mL) | Tmax (min) | AUC (uU·h/mL) | Bioavailability (%) |
|---|---|---|---|---|
| **Insulin solution** | 4.9 ± 1.8 | 76.3 ± 54.9 | 5.7 ± 2.0 | 0.2 ± 0.1 |
| **+ L-Penetratin** | | | | |
| **0.05 mM** | 8.1 ± 2.4 | 30.0 ± 15.0 | 9.3 ± 1.0 | 0.3 ± 0.0 |
| **0.1 mM** | 6.3 ± 1.6 | 11.7 ± 1.7 | 6.8 ± 0.4 | 0.2 ± 0.0 |
| **0.2 mM** | 110.0 ± 21.2* | 10.0 ± 0.0 | 28.5 ± 4.8** | 1.0 ± 0.2** |
| **0.5 mM** | 620.0 ± 312.2 | 13.3 ± 1.3 | 181.9 ± 106.7 | 6.1 ± 3.6 |
| **1 mM** | 1061.5 ± 198.5* | 15.0 ± 0.0 | 512.8 ± 145.7* | 17.3 ± 4.9* |
| **2mM** | 1416.1 ± 593.8 | 23.3 ± 6.7 | 1049.7 ± 495.1 | 35.4 ± 16.7 |
| **+ D-Penetratin** | | | | |
| **0.05 mM** | 33.3 ± 9.6 | 15.0 ± 0.0 | 17.3 ± 9.3 | 0.6 ± 0.3 |
| **0.1 mM** | 97.7 ± 52.7 | 18.3 ± 6.0 | 43.5 ± 29.1 | 1.5 ± 1.0 |
| **0.2 mM** | 146.1 ± 60.5 | 15.0 ± 0.0 | 60.1 ± 26.1 | 2.0 ± 0.9 |
| **0.5 mM** | 52.8 ± 11.5 | 30.0 ± 0.0 | 26.6 ± 4.8** | 0.9 ± 0.2** |
| **1 mM** | 10.0 ± 2.1 | 33.8 ± 9.4 | 8.1 ± 2.6 | 0.3 ± 0.1 |
| **2 mM** | 0.8 ± 0.1 | 73.3 ± 46.5 | 0.9 ± 0.4 | 0.0 ± 0.0 |

Data: mean ± S.E. (n=3 or 4).
Cmax: the maximum concentration; Tmax: the time to reach the Cmax; AUC: the area under the curve.
*$p$<0.05, **$p$<0.01: Significant difference to corresponding "Insulin solution".

### 3.4. Effect of intestinal fluid on the aggregation of insulin and penetratin

Figure 9 shows photographs of a physical mixture solution of insulin (132 μM, the same concentration as the administration solution) and L- or D-penetratin (1 mM). Aggregation began immediately after mixing insulin with L- and D-penetratin, and the mixed solution became cloudy. The turbidity of the solution did not change over time and seemed to be stable. However, in the case of the insulin and L-penetratin solution, the turbidity was quickly diminished by adding intestinal solution, and the solution

became clear after 60 min, as shown in Fig. 9A. In contrast, the turbidity of the insulin and D-penetratin solution remained after adding intestinal solution even after 60 min, as shown in Fig. 9B.

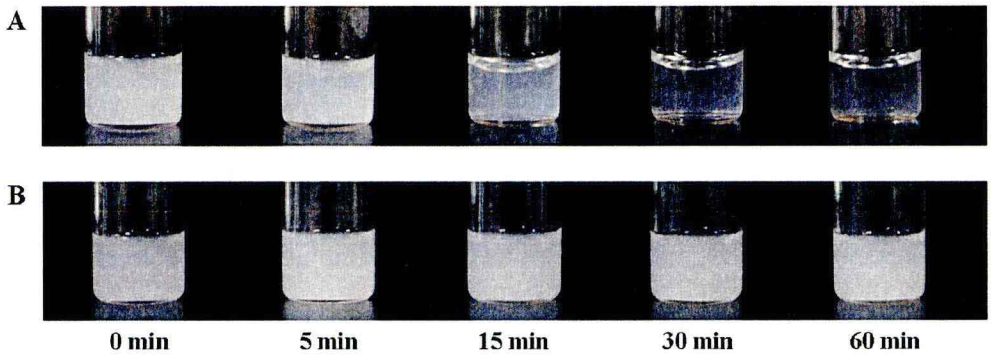


Fig. 9. Effect of intestinal enzyme fluid on precipitation induced by the mixing of insulin (132 μM) and L- or D-penetratin (1 mM). Top photographs: L-penetratin, Bottom photographs: D-penetratin.

## 4. Discussion

For the strategies using CPPs, covalent binding between therapeutic agents and permeable peptides is essential, and in many cases, drugs and permeable peptides are cross-linked in a 1:1 molecular ratio. In contrast, I proposed an approach using a CPP without intermolecular crosslinking, and I succeeded in achieving efficient delivery of insulin from the intestine to the systemic circulation using a typical CPP, oligoarginine. In this noncovalent delivery approach, the absorption enhancing ability of the CPP may be dependent on the binding affinity of the CPP to insulin, based on electrostatic and/or hydrophobic interactions. Therefore, this approach required relatively high doses of the CPP. In this chapter, the effects of some CPPs on ileal insulin absorption were examined to identify functional peptides that enhanced intestinal insulin absorption more effectively.

As shown in Table 8, intestinal insulin absorption was significantly enhanced by R8, penetratin, pVEC, and RRL helix. R8 is an artificial CPP composed of eight residues of arginine; penetratin is derived from *Drosophila* Antennapedia homeoprotein; pVEC is derived from murine vascular endothelial cadherin; and RRL helix is α-helical amphipathic model peptide consisting of arginine and leucine. Furthermore, the pharmacological activity of insulin remained after coadministration with these peptides because a strong hypoglycemic reaction was observed (data not shown). However, the effectiveness of the L- and D-forms of peptides in enhancing insulin absorption differed among peptides. In the case of R8, the D-form of the peptide had a stronger ability to enhance intestinal insulin absorption than the L-form. In contrast, the other three peptides exerted effects that were more significant when the L-forms were applied. In the literature, L- and D-oligomers of arginine have been reported to have similar abilities

to internalize into a cell [31]. However, the sensitivity of each oligomer to peptidase and protease is quite different, and generally peptides composed of D-form amino acids are far more resistant to enzymatic degradation than peptides composed of L-form amino acids [56,57]. Therefore, in the case of D-R8, its high stability in the presence of intestinal enzymes may result in the strong enhancement effect on ileal insulin absorption. In contrast, my results demonstrated that L-penetratin, L-pVEC, and L-RRL helix enhanced intestinal insulin absorption more strongly than their D-forms. Furthermore, the ability of L-penetratin to enhance insulin absorption was greater than that of D-R8, and L-penetratin had the most significant effects on enhancing the bioavailability of insulin among the peptides used in the present study.

Meanwhile, in a mixture of CPP and insulin, precipitation was induced in the solution at high concentrations of CPPs. Cationic peptides interact with negatively charged proteins, and consequentially aggregates are formed by electrostatic neutralization [58]. In agreement with the literature, when high concentrations of CPPs were added to an insulin solution in the present experiments, turbidity of the solution was observed, indicating the formation of aggregates. In the case of penetratin, aggregation began when L- or D-peptides at a concentration of 0.5 mM or more were added into the insulin solution. Therefore, at a CPP concentration of 0.5 mM or more, it may be difficult to increase insulin absorption because the aggregates have visible size and may not be able to permeate the intestinal lumen to reach the circulation. I speculate that the fractions of insulin and CPP that bound to each other but did not form bigger aggregates contributed to the enhancing effect of L-penetratin on intestinal insulin absorption.

As shown in Fig. 8 and Table 10, L- and D-penetratin-enhanced intestinal insulin

absorption was dependent on the applied penetratin concentration up to 0.5 mM. In contrast, different effects were observed when L- and D-penetratin were applied at concentrations over 0.5 mM. Although L-penetratin significantly enhanced insulin absorption at concentrations greater than 0.5 mM, the absorption enhancing ability of D-penetratin decreased at concentrations exceeding 0.5 mM. To explain these phenomena, the formation of aggregates after mixing insulin and penetratin was examined in the presence of intestinal enzyme fluid. As shown in Fig. 9, L-penetratin aggregates gradually disappeared in the presence of intestinal fluid, and the solution became almost clear after 60 min. In contrast, D-penetratin aggregates remained throughout the study period even in the presence of intestinal fluid. This implies that L-penetratin aggregates were degraded by intestinal enzymes because of the low resistance of the L-form of the peptide to enzymatic degradation. On the other hand, the internalization efficiency of penetratin is retained even when its sequence is partially modified [59], suggesting that the fractionated penetratin may have internalization ability. In other words, all amino acid sequences of penetratin might not be prerequisite on the cellular internalization of the peptide, therefore, the enzymatic decomposition products of L-penetratin may enhance insulin intestinal absorption. In contrast, the enzymatic decomposition products of L-R8 may not have such effects. In fact, the number of arginine residues in L-R8 is important for the internalization efficiency of the molecule, and the effects of this CPP dramatically decrease with the decrease in arginine residues [31].

## 5. Conclusions

L-penetratin acted as the most effective bioavailability enhancer for intestinal insulin among the 10 different CPPs used in the present study. The results of the LDH leakage study suggested that undesirable toxic effects on the intestinal mucosa were not caused by administration of L-penetratin. These results suggest that L-penetratin has great potential as a powerful tool for insulin delivery across intestinal absorption barriers. To evaluate the further potential of penetratin as a bioenhancer, it will be necessary to examine its effects on the bioavailability of other peptide and protein drugs that have different electrical charges in physiological pH. In addition, my results suggest that the effectiveness of CPPs in enhancing intestinal insulin absorption varies depending on the binding affinity between insulin and each CPP, the applied concentration of CPP to insulin, and the chirality of amino acids within each CPP. Therefore, further study is needed to determine affinity constants between insulin and CPP molecules and clarify the enhancement mechanisms of CPPs.

# Chapter 3

# Permeation characteristics of oligoarginine through intestinal epithelium

## 1. Introduction

In the previous chapters, I have reported that a typical CPP, oligoarginine, enhances the intestinal absorption of the peptide drug, insulin. Because oligoarginine has negligible adverse effects on the intestinal mucosa, it is potentially a safe delivery system. Moreover, my strategy does not need covalent conjugation between drug and CPP unlike many approaches in other laboratories. However, the mechanisms underlying its enhancement of intestinal drug absorption are unknown. In addition, although some publications refer to the epithelial permeation of CPPs [60-64], there is no information about the permeation characteristic of CPPs, especially oligoarginine, through biological intestinal membranes.

In this chapter, I first evaluated the permeability of isolated rat intestinal epithelial membranes to oligoarginine itself under various conditions, including low temperature, the presence of heparin, and pretreatment with hyaluronidase, to clarify the permeation characteristics of oligoarginine across the intestinal epithelial membrane. Beside my methodology based on physically mixed solution of drug and CPP, there is a publication relevant to method based on covalent binding which achieve the effective insulin permeation [49]. However, this was undertaken by using Caco-2 cells, not biological membrane. Therefore, the effects on the biological ileal permeation of a peptide drug after its coincubation with oligoarginine and the absorption of an oligoarginine-introduced peptide derivative by ileal segments were examined to evaluate the usefulness of an oral delivery system based on oligoarginine. Leuprolide, a relatively small peptide, was used and was conjugated to oligoarginine.

## 2. Materials and Methods

### 2.1 Materials

Leuprolide acetate salt, L-R6 (RRRRRR; R, L-arginine), D-R6 (rrrrrr; r, D-arginine), fluorescein-labeled D-R6 (FL-D-R6), and lyophilized hyaluronidase (EC 3.2.1.35; type IV-S from bovine testes, 56 kDa, 1370 IU/mg solid) were purchased from Sigma-Aldrich Co. (St Louis, MO, USA). Heparin sodium was purchased from Wako Pure Chemical Industries, Ltd (Osaka, Japan). The leuprolide-D-R6 conjugate (amino acid sequence shown in Table 11) was synthesized by the Peptide Institute, Inc. (Osaka, Japan). All other chemicals were of analytical grade and are commercially available.

Table 11. Molecular weights and amino acid sequences of leuprolide and the leuprolide-D-R6 conjugate

| Peptides | Mw | Sequence |
|---|---|---|
| **Leuprolide** | **1209** | **XHWSYlLRP-NHCH$_2$CH$_3$** |
| **Leuprolide-D-R6** | **2636** | **XHWSYlLRPrrrrrrk(FITC)-NH$_2$** |

X: pyroglutamic acid, H: histidine, W: tryptophan, S: serin Y: tyrosine l: D-leucine, L: leucine, R: arginine, P: praline, r: D-arginine k: D-lysine.

### 2.2. Animals

Male Wistar rats weighing 180–220 g were purchased from Sankyo Laboratory Service (Tokyo, Japan). The experiments using animals were performed at Hoshi University and complied with the regulations of the Committee on Ethics in the Care and Use of Laboratory Animals. The animals were housed in rooms maintained at 23 ± 1 °C and 55 ± 5% relative humidity, and were allowed free access to water and food during acclimatization. All animals were fasted for 24 h before the experiments.

### 2.3. In vitro permeation study

In vitro permeation experiments were performed with an Ussing chamber (Nihon-Kohden Tokyo, Japan) using rat ileal segments, without Peyer's patches.

#### 2.3.1. FL-D-R6 permeation experiments

Following anesthetization with an intraperitoneal injection of sodium pentobarbital (50 mg/kg; Dainippon Sumitomo Pharm Co., Ltd., Osaka, Japan), the rats were restrained in a supine position on a thermostatically controlled board at 37 °C. Briefly, the ileum was exposed after a small midline incision had been carefully made in the abdomen. Immediately thereafter, a segment of the ileum was removed, opened along the mesenteric border, and carefully washed with ice-cold (bicarbonate-buffered) Krebs–Ringer solution (pH 7.4) containing 0.001% methylcellulose to prevent the adsorption of the peptide to the surface of the chamber or to the container. The Krebs–Ringer solution contained (in mM): 108.0 NaCl, 11.5 D-glucose, 15.0 $NaHCO_3$, 4.7 KCl, 1.8 $NaH_2PO_4$, 0.4 $KH_2PO_4$, 1.2 $MgSO_4$, 1.25 $CaCl_2$, 4.9 Na-glutamate, 5.4 $Na_2$-fumarate, and 4.9 Na-pyruvate. The flattened membrane sheets were then mounted in an Ussing chamber, exposing a surface area of 1 $cm^2$. Both the mucosal side (donor side) and the serosal side (receiver side) were filled with 5.0 mL of Krebs–Ringer solution continuously bubbled with a gas mixture of 95% $O_2$ and 5% $CO_2$. The temperature was maintained at 37 or 4 °C during the permeation of FL-D-R6 across the ileal membrane. The intestinal membranes were then allowed to equilibrate for 20 min. FL-D-R6 was prepared with Krebs–Ringer solution. After the equilibration period, the permeation experiment was started by replacing 0.5 mL of the solution on the mucosal side with an equal volume of FL-D-R6 solution, and the final concentration on the donor

side was adjusted to 200 μM FL-D-R6. At a predetermined time, samples (400 μL) were taken from the serosal side and immediately replaced with an equal volume of Krebs–Ringer solution. To evaluate the contribution of the adsorption of FL-D-R6 to cell-surface proteoglycans to the permeation of FL-D-R6 across the ileal mucosal membrane, FL-D-R6 was coincubated with heparin (1 mg/mL) on the donor side. The permeation experiment was also performed using ileal membrane pretreated with hyaluronidase to evaluate the contribution of the mucus/glycocalyx layers lying on the epithelial cells to the ileal permeation of FL-D-R6. The treatment with hyaluronidase was performed by exposing the ileal segments to 1.0 mL of hyaluronidase solution ($1.92 \times 10^5$ U/mL) dissolved in phosphate-buffered saline (PBS) for 30 min after the intestinal contents had been flushed out. After exposure, the segments were carefully rinsed with 20 mL of PBS at 37 °C, and the segments were then used in the permeation experiment. The FL-D-R6 concentration was measured using a microplate luminometer (Mithras LB940, Berthold Japan, Tokyo, Japan) at excitation and emission wavelengths of 485 and 535 nm, respectively.

The steady-state flux ($J_{ss}$) was calculated from the linear portion of the cumulative flux-vs-time curve. The apparent permeability coefficient ($P_{app}$) of each compound was calculated with the equation:

$$P_{app} = J_{ss}/C \qquad \text{(Eq. 1)}$$

where C is the initial donor concentration.

The amount of tissue-associated FL-D-R6, which is the total amount of the peptide internalized to the inside of the membrane and the peptide bound to the surface of the

membrane, was determined by measuring the fluorescence intensity of the homogenate of the ileal membrane sheet after the in vitro permeation experiment. At the end of the 3 h permeation experiment, the ileal tissue was removed from the Ussing chamber. The area of the ileal membrane exposed to the solution was excised and rinsed thoroughly twice with 30 mL of Krebs–Ringer solution to remove any unbound FL-D-R6. The washed tissue was homogenized with a Teflon homogenizer in fresh Krebs–Ringer solution, and centrifuged at 200 × g for 10 min at 4 °C to remove any tissue fragments. The supernatants were analyzed after each centrifugation with a microplate luminometer at excitation and emission wavelengths of 485 and 535 nm, respectively.

### 2.3.2. Leuprolide permeation experiments

The ileal segments were removed and treated with the same process as described above for the FL-D-R6 permeation study. The muscle layers were then stripped away, and the flat membranes were mounted in an Ussing chamber that exposed 0.1 $cm^2$ of tissue to 1.0 mL of Krebs–Ringer solution continuously bubbled with 95% $O_2$–5% $CO_2$ on each side, at 37 °C. The intestinal membranes were then allowed to equilibrate for 20 min. Leuprolide, L-R6, and D-R6 were prepared with Krebs–Ringer solution. After an equilibration period, the permeation experiment was started by replacing the solution on the mucosal side with an equal volume of leuprolide and L-R6 or D-R6 solutions, and the final concentrations on the donor side were adjusted to 125 μM for leuprolide and 125 μM for L-R6 and D-R6. At predetermined times, samples (200 μL) were taken from the serosal side, and each was immediately replaced with an equal volume of Krebs–Ringer solution. The leuprolide concentration was measured using a leuprolide enzyme-linked immunosorbent assay (ELISA) kit (Endocrine Technologies Inc.,

Fircrest St, Newark, CA, USA).

To assess tissue viability during the series of experiments, the spontaneous transmucosal potential difference (PD) and the short-circuit current ($I_{sc}$) were monitored simultaneously at the start and end of each test period. The values for membrane resistance (Rm) were calculated as $PD/I_{sc}$, based on Ohm's law. These were corrected by eliminating the offset voltage between the electrodes and the series fluid resistance, which was determined before each experiment using the same bathing solutions but without the membranes mounted in the chamber. The Rm values for the intestinal membrane in the steady state were greater than 30 $\Omega/cm^2$. The course of Rm during the test period did not differ in the presence or absence of R6, indicating that the viability of the intestinal membrane was maintained in the presence of R6.

**2.4. In situ loop absorption study**

This study was performed in the similar procedures as described in Chapter 1. After the surgical process, leuprolide (0.25 mL) or leuprolide-D-R6 solution (0.25 mL) at 37 °C was directly administered to an ileal loop (6 cm) made from a rinsed segment (10 cm). The concentration of both drug solutions was 10 mM, so that the doses of leuprolide and leuprolide-D-R6 were 12.5 μmol/kg body weight. Blood samples (0.3 mL) were withdrawn via the jugular vein before the administration and at 30, 60, 120, 180, 240, 300, and 360 min after the administration of the drug. Additional intraperitoneal injections of sodium pentobarbital (12.5 mg/kg) were necessary every 1 h after the administration of the drug to maintain anesthesia. The plasma was separated by centrifugation at 13,400 × *g* for 1 min and kept under refrigeration until analysis. The efficiency of leuprolide and leuprolide-D-R6 absorption was evaluated by measuring the

plasma testosterone concentration because it is difficult to determine the plasma leuprolide-D-R6 concentration with an enzymatic immunoassay-based system. The increase in the plasma testosterone concentration is dependent on the increase in the plasma leuprolide concentration and is thus a biological index of absorbed leuprolide. These concentrations were determined using the Testosterone ELISA Kit for Rodents (Endocrine Technologies Inc., Fircrest St, Newark, CA, USA). The total area under the testosterone concentration curve (AUC) from time 0 to 6 h was estimated from the sum of successive trapezoids between each data point.

To confirm the biological activity of leuprolide-D-R6 compared with unconjugated leuprolide, leuprolide-D-R6, and leuprolide were administered via an i.v. route. In a similar manner to the in situ absorption study, the ileal segments were gently rinsed with PBS. Leuprolide (200 μL) or leuprolide-D-R6 solution (200 μL) was administered via the jugular vein. The concentration of both drug solutions was 150 nM, so that the doses of leuprolide and leuprolide-D-R6 were 150 pmol/kg body weight. Blood samples (0.3 mL) were withdrawn from the jugular vein before the administration and at 30, 60, 90, 120, 180, 240, and 300 min after the administration of the drug. As described above, plasma testosterone levels were determined and the AUC from time 0 to 6 h was estimated.

### 2.5. Statistical analysis

Each value is expressed as the mean ± standard deviation (S.D.). For group comparisons, analysis of variance (ANOVA) with a one-way layout was applied. The mean values were evaluated by Student's unpaired $t$ test and $p < 0.05$ was considered significant.

## 3. Results

### 3.1. Permeation characteristics of oligoarginine through the ileal membrane

Figure 10 and Table 12 show the time profiles of FL-D-R6 permeation through the isolated ileal membranes, and the parameters of its permeation and tissue distribution under various conditions, respectively. At 37 °C, simulating biological conditions, FL-D-R6 permeated gradually after a short lag time and its $P_{app}$ was 7.26 × $10^{-8}$ cm/s. The peptide that was internalized into the intestinal tissue but did not permeate to the opposite side was 181 nmol/g membrane. At 4 °C, at which temperature energy-dependent active transport across biological membranes is abolished [65,66], $P_{app}$ and the tissue-distributed amount of FL-D-R6 decreased to 0.82 × $10^{-8}$ cm/s and 133 nmol/g, respectively. Moreover, these parameters decreased to 1.60 × $10^{-8}$ cm/s and 21.7 nmol/g, respectively, in the presence of heparin, which was negatively charged and used to inhibit the electrostatic binding of positive molecules to the negatively charged proteoglycans on cell membrane surface. In contrast, these parameters increased slightly in the presence of hyaluronidase, which was used in the pretreatment to diminish the glycocalyx layer on the membrane, which functions as one of major permeation barriers for hydrophilic macromolecules and exogenous pathogens.

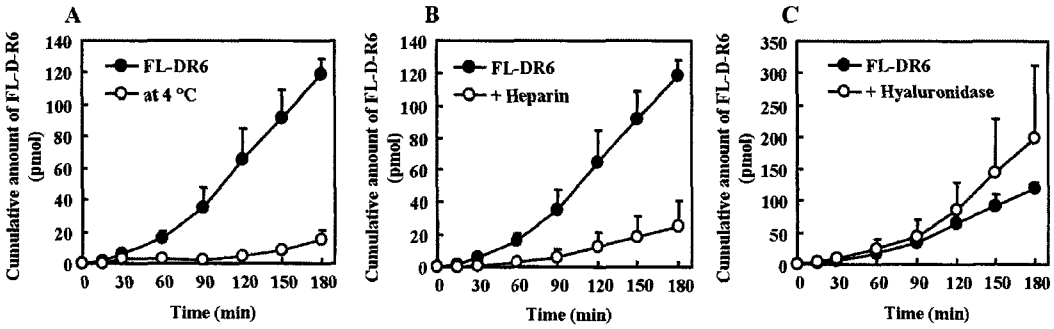


Fig. 10. Time profiles of FL-D-R6 permeation across rat ileal membranes under various conditions. A: low temperature (4 °C); B: presence of heparin; C: pretreatment with hyaluronidase. Each data represents the mean ± S.D. (n=3).

Table 12. Apparent permeability coefficients and tissue distributions of FL-D-R6 during the rat permeation experiment under various conditions

| | Apparent permeability coefficient, $P_{app}$ ($\times 10^{-8}$ cm/s) | Tissue distributed amount (nmol/g) |
|---|---|---|
| **Biological condition (37 °C)** | **7.3 ± 0.4** | **181 ± 26** |
| **Low temperature (4 °C)** | **0.8 ± 0.3*** | **133 ± 37** |
| **With Heparin** | **1.6 ± 1.0*** | **22 ± 8*** |
| **Hyaluronidase pretreatment** | **12.5 ± 7.3** | **240 ± 31** |

Data: mean ± S.D. (n=3).
*$p<0.05$ against "biological condition (37 °C)".

## 3.2. Effect of oligoarginine on the permeation of leuprolide through the ileal membrane

Figure 11 and Table 13 show the time profiles of leuprolide permeation through isolated ileal membranes and the permeation parameters, respectively. In these permeation experiments, leuprolide and L- or D-R6 were applied as a physically mixed solution. However, there was no difference in leuprolide permeation with or without L- or D-R6.

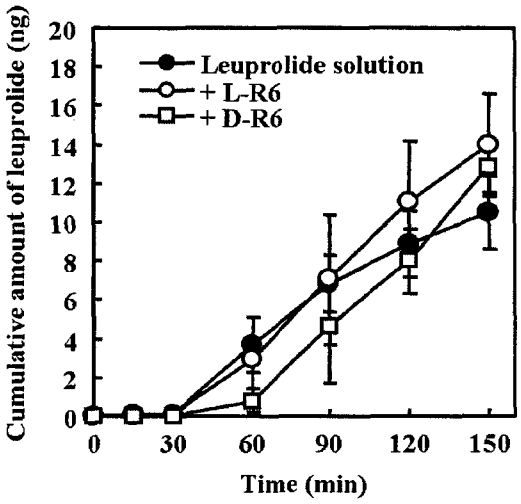


Fig. 11. Time profiles of leuprolide permeation through rat ileal membranes in the absence or presence of L-R6 or D-R6. Each data represents the mean ± S.D. (n=3–4).

Table 13. Apparent permeability coefficients of leuprolide during the rat ileal permeation experiment in the absence or presence of L-R6 or D-R6

| | **Apparent permeability coefficient, $P_{app}$ ($\times 10^{-8}$ cm/s)** |
|---|---|
| **Leuprolide solution** | **10.6 ± 0.2** |
| **+ L-R6** | **13.3 ± 2.6** |
| **+ D-R6** | **12.1 ± 1.2** |

Data: mean ± S.D. (n=3–4).

### 3.3. Determination of the biological activity of the leuprolide-D-R6 conjugate relative to that of the original leuprolide

The biological activity of leuprolide is expressed in terms of its testosterone-stimulatory effect. The AUC of testosterone 6 h after the i.v. administration

of 150 pmol/kg leuprolide was 138.4 ± 68.8 ng·min/mL (time profiles not shown). In contrast, the AUC after the i.v. administration of the leuprolide-D-R6 conjugate was 50.0 ± 28.0 ng·min/mL. Therefore, the relative biological activity of the leuprolide-D-R6 conjugate, which was calculated by dividing the activity of leuprolide-D-R6 by that of the original leuprolide, was approximately 0.36.

### 3.4. Intestinal absorption of the leuprolide-D-R6 conjugate

Figure 12 shows the effect of the conjugation of leuprolide and D-R6 on the absorption of leuprolide after in situ ileal administration. The amount of absorbed leuprolide was determined by measuring the resultant testosterone concentration. The testosterone concentration after the administration of leuprolide-D-R6 was also corrected with the equation:

$$Cc = Ct/R \qquad \text{(Eq. 2)}$$

where Ct is the actual plasma testosterone concentration at time t, R is the relative biological activity of the leuprolide-D-R6 conjugate in the i.v. experiments (0.36), and Cc is the corrected plasma testosterone concentration after the administration of the leuprolide-D-R6 conjugate.

The plasma testosterone concentrations after the administration of leuprolide showed a response pattern consistent with the single-dose study of leuprolide. The increase in the plasma testosterone concentration after the ileal administration of leuprolide was diminished by conjugating D-R6 to leuprolide. Table 14 summarizes the pharmacokinetic parameters derived from the testosterone concentration–time profiles

following the in situ administration of the original leuprolide or the leuprolide-D-R6 conjugate to ileal segments. There was no significant difference in the AUCs after the administration of leuprolide-D-R6 and the administration of the original leuprolide.

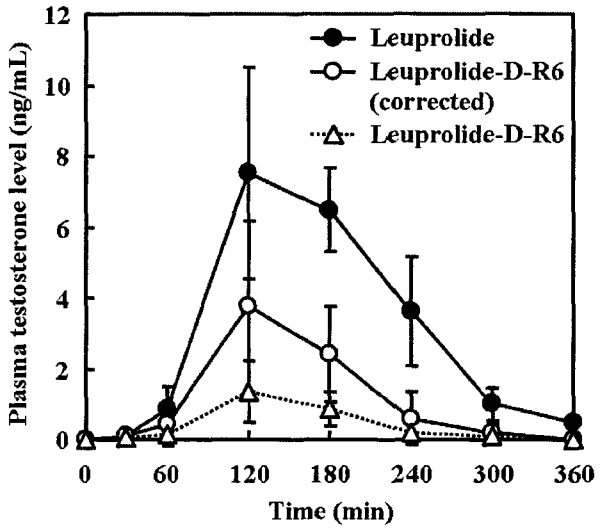


Fig. 12. Plasma testosterone concentrations vs time profiles after the in situ application of leuprolide (●) or the leuprolide-D-R6 conjugate (○) to rat ileal segments. The plasma testosterone concentration after the conjugate was administered was calculated from the actual concentration (△) and its biological activity. Each data represents the mean ± S.D. (n=3).

Table 14. Pharmacological parameters after the in situ administration of leuprolide–D-R6 conjugate to rat segments

| | Cmax (ng/mL) | Tmax (min) | AUC (ng·h/mL) |
|---|---|---|---|
| **Leuprolide** | **8.3 ± 2.2** | **140.0 ± 34.6** | **18.8 ± 5.6** |
| **Leuprolide-D-R6 conjugate (corrected)** | **3.8 ± 2.4** | **120.0 ± 0.0** | **7.1 ± 5.2** |

These parameters were calculated from the time profiles of plasma testosterone concentrations.
Data: mean ± S.D. (n=3).
Cmax: the maximum testosterone concentration, Tmax: the time to reach the Cmax, AUC: the area under the curve.

## 4. Discussion

In the previous chapters, I demonstrated that the intestinal absorption of insulin, a peptide drug, was improved by its coadministration with various CPPs into the ileal loop. My approach, which was to administer a physical mixture of insulin and oligoarginine, is distinct from the intracellular delivery using a conjugate of the drug and a CPP used in many laboratories. However, the mechanisms underlying its enhancement of intestinal drug absorption are unknown. In addition, there is negligible information about the permeation characteristics of CPPs through the biological intestinal membranes. Therefore, the permeation of oligoarginine, used in Chapter 1, was first examined to obtain the information relevant to mechanisms on the enhancement of intestinal drug absorption by oligoarginine.

In this study, the amount of oligoarginine that permeated to the serosal side and the tissue-distributed amount of oligoarginine (the total adsorbed and internalized oligoarginine) were measured to evaluate its permeation characteristics. FL-D-R6, which is six polymerized D-arginines labeled with fluorescein, was used to eliminate the enzymatic degradation of oligoarginine, because generally peptides composed of D-form amino acids are far more resistant to enzymatic degradation than peptides composed of L-form amino acids [56]. The permeation of FL-D-R6 was significantly reduced at 4 °C compared with its permeation at 37 °C (Fig. 10A and Table 12), suggesting that the internalization of oligoarginine into the cell or its permeation through the intestinal epithelial membrane is mediated by an energy-dependent transport pathway. The tissue distribution of FL-D-R6 was only slightly reduced at 4 °C, implying that the distribution of the peptide is not affected by the reduction in the incubation temperature, indicating the energy-independent attachment of FL-D-R6 to the mucosal membrane. Heparin also

significantly diminished the permeation of FL-D-R6 through and its distribution in the intestinal membrane (Fig. 10B and Table 12), suggesting that the free FL-D-R6 fraction was decreased by the binding of negatively charged heparin to FL-D-R6. Consequently, the electrostatic adsorption of FL-D-R6 to proteoglycans on the epithelial membrane surface was abolished. These results on intestinal biological membranes are consistent with the results of other studies of cultured cell lines, which showed that the uptake of CPPs by cells is mediated by their adsorption to the cell surface and their subsequent internalization via endocytosis. In contrast, treatment with hyaluronidase, which reduces the mucus/glycocalyx layer on the intestinal epithelial membrane, slightly increased the permeability of the mucosal membrane and the tissue distribution of FL-D-R6 (Fig. 10C and Table 12). I speculate that the presence of the mucus/glycocalyx layer is not involved in the permeation of oligoarginine. In short, little oligoarginine adsorbed to this layer. Proteoglycans anchored on the cell surface, which remain on the cell surface after treatment with hyaluronidase, are essential for the permeation of oligoarginine through the membrane, rather than the mucus/glycocalyx layer. However, the release of internalized oligoarginine across the basal membrane may be difficult even though its internalization into the intestinal epithelium is achieved by above-mentioned mechanisms, because the permeation of FL-D-R6 was far lower than that of 4-kDa dextran, FD-4 (data not shown). Thus, the internalization of oligoarginine on the apical membrane may induce the increased uptake of peptide drug into intestinal epithelium and contribute to the enhancement of intestinal drug absorption.

During the submission of my work based on physically mixed solution of drug and CPP as mentioned above, it became known that permeation of insulin through intestinal epithelium was improved by conjugating with Tat peptide [49]. However, this

examination was performed using Caco-2 cells, not biological membrane. Therefore, the effects on the biological ileal permeation of leuprolide, a peptide drug, after its coincubation with L- or D-R6 and the absorption of D-R6-introduced peptide derivative by ileal segments were examined to evaluate the usefulness of an oral delivery system based on oligoarginine. First, leuprolide was physically mixed with L- or D-R6 and then applied to the donor side of the Ussing chamber, because the ileal absorption of insulin was enhanced by its coadministration with L- or D-R6 in Chapter 1. However, the permeation of leuprolide was not affected by L- or D-R6 (Fig. 11 and Table 13). These results are consistent with results presented in Chapter 1 in that only the intestinal absorption of a negatively charged molecule, insulin, was enhanced by coadministration with oligoarginine, whereas that of positively charged IFN-β and neutral FD-4 was not. This study suggests that positively charged leuprolide does not interact with positively charged oligoarginine to form an electrostatic complex. I next covalently conjugated leuprolide to D-R6. However, the absorption of the leuprolide-D-R6 conjugate was lower than that of the original leuprolide (Fig. 12 and Table 14). I speculated that the leuprolide-D-R6 conjugate was taken up by the ileal epithelial cells based on the above-mentioned results of the FL-D-R6 permeation study and other studies of protein–CPP or DNA–CPP conjugates in intracellular delivery [36,67]. However, the permeation of the leuprolide-D-R6 conjugate across the serosal membrane was limited by its high molecular weight and its polarity when conjugated to D-R6. In fact, it has been reported that internalized CPPs have difficulty escaping to the outside of the cell [60,61]. It has also been demonstrated that an increase in molecular weight diminished the permeation of leuprolide via the paracellular pathway, which is the primary route of leuprolide permeation [68,69]. As mentioned above, the main route for the permeation

of leuprolide shifted from the paracellular pathway to the active transcellular pathway by conjugating it to D-R6. However, the low permeation of the leuprolide-D-R6 conjugate across the serosal membrane limited its final release into the circulation. In contrast, other studies have indicated that the permeation of Tat–insulin through a Caco-2 monolayer was higher than that of the original insulin [49]. The discrepancy between my present results and other published data is attributable to differences in the permeation characteristics of these drugs through the intestinal epithelium. It is possible that the increased internalization of insulin into epithelial cells resulted directly in the enhanced permeation to the receiver side because the paracellular transport of insulin is limited by its molecular weight, which is higher than that of leuprolide (insulin, 5807 Da vs leuprolide, 1209 Da). In contrast, I speculate that insulin physically mixed with oligoarginine interacts electrostatically with the oligoarginine under the conditions used, and the complex of these molecules enters epithelial cells. The insulin is released from the complex in the cytoplasm and escapes into the circulation. Thus, the use of a physically mixed solution of insulin and oligoarginine is considered to be a more potentially successful and convenient strategy. However, the fact that oligoarginine enhances intestinal drug absorption, depending on the electrostatic characteristics of each molecule, has not been demonstrated. It will be necessary to determine the affinity between oligoarginine and each drug to establish the optimal use of oligoarginine for intestinal drug delivery.

## 5. Conclusions

This study was undertaken to clarify the permeation characteristics of oligoarginine through the intestinal epithelial membrane. The internalization of oligoarginine into the intestinal tissue was mediated by its adsorption to cell-surface proteoglycans and its subsequent transduction via an energy-dependent pathway. The release of oligoarginine across basal membrane may be limited, suggesting that the internalization of oligoarginine on the apical membrane rather than its permeation through epithelial membrane may contribute to the enhancement of intestinal drug absorption. Although I used a strategy based on the characteristics of oligoarginine to improve the intestinal permeation of leuprolide, oligoarginine had no stimulatory effect on the intestinal permeation of leuprolide either when leuprolide and oligoarginine were administered together or when an oligoarginine derivative of leuprolide was administered. The findings of this chapter and previous chapters indicate that the strategy using oligoarginine to improve intestinal drug permeation requires an intermolecular interaction, such as an electrostatic interaction, between the drug and oligoarginine, and in some case a covalent linkage between the macromolecular drug and oligoarginine may hamper the ability of oligoarginine to enhance intestinal epithelial permeation of therapeutic peptides and proteins.

# Chapter 4

# Importance of intermolecular interaction on the improvement of intestinal therapeutic peptide/protein absorption using cell-penetrating peptides

## 1. Introduction

In the previous chapters, the sufficient intestinal absorption of therapeutic peptides and proteins has been achieved by more convenient methods in which a physical mixture of drug and CPP was administered. This methodology differs from conventional approaches using CPPs in which a conjugation process between macromolecules and CPPs is essential for their effective internalization. However, the reasons why physical mixtures of drug and CPP significantly enhance intestinal drug absorption are unclear. In a Chpater 1, the effects of the CPP on intestinal drug absorption were described as different, depending on the physical properties of the model drug used. For instance, in an in situ ileal loop absorption study, the ileal absorption of insulin (a peptide possessing negative charge at physiological pH) was significantly increased by coadministration of R6; however, the absorption of IFN-β (a large protein possessing weak positive charge at physiological pH) and neutralized FD-4 was only slightly affected by coadministration of R6. In addition, in an in vitro permeation study using isolated rat ileal membrane, the ileal permeation of leuprolide, a peptide possessing positive charge, was unchanged in the presence of R6 as shown in Chapter 3. Thus, only absorption of negatively charged macromolecules was improved by this methodology, wherein a target molecule was physically mixed with a positively charged CPP. Therefore, I hypothesized that the electrostatic interaction between each drug and CPP may be related to the phenomenon whereby the enhancing effect of the CPP on the intestinal drug absorption varies depending on the kind of drug. Although the involvement of an electrostatic interaction between CPP and drug to mediate the enhancing effect of the CPP on the drug permeation through cell membranes has been proposed, until now, there has been no report to provide unambiguous evidence for this

possibility.

In this chapter, to verify the electrostatic-interaction hypothesis, I evaluated the relationship between the ability of the CPP to enhance intestinal drug absorption, and the intermolecular interaction of drug and CPP. First, the binding characteristics between D-R8, a typical oligoarginine consisting of only D-form amino acids, and several peptide drugs possessing different isoelectric points were analyzed by surface plasmon resonance (SPR)-based measurement. The peptides used in this examination are shown in Table 15. The effects of D-R8 on the intestinal absorption of these peptide drugs were examined to clarify the relevance of intermolecular binding. The alteration of binding characteristics between peptide drugs and D-R8 and the consequent changes in absorption enhancement were evaluated in detail for insulin and glucagon-like peptide-1 (GLP-1).

Table 15. Molecular characteristics of peptide drugs used in the present study

| | Mw | pI | Polarized amino acids |
|---|---|---|---|
| **Gastrin I, Human** | **2098** | **2.8** | **Glu: 4, Asp: 1** |
| **Exendin-4** | **4187** | **4.5** | **Glu: 5, Asp: 1, Arg: 1, Lys: 2** |
| **Oxytocin** | **1007** | **5.2** | |
| **Insulin** | **5808** | **5.3** | **Glu: 4, Arg: 1, Lys: 1** |
| **GLP-1 (7-36)** | **3298** | **5.5** | **Glu: 3, Asp: 1, Arg: 1, Lys: 2** |
| **Leucine Enkephalin** | **556** | **5.7** | |
| **Thyrotropin Releasing Hormone** | **362** | **7.9** | |
| **Angiotensin I** | **1296** | **8.0** | **Asp: 1, Arg: 1** |
| **[Arg$^8$]-Vasopressin** | **1084** | **8.3** | **Arg: 1** |
| **Calcitonin, Salmon** | **3492** | **9.0** | **Glu: 1, Arg: 1, Lys: 2** |
| **Somatostatin** | **1638** | **9.2** | **Lys: 2** |
| **Leuprolide** | **1209** | **9.7** | **Arg: 1** |
| **Luteinizing Hormone-Releasing Hormone** | **1182** | **9.7** | **Arg: 1** |
| **Mastoparan** | **1479** | **10.9** | **Lys: 3** |
| **Adrenocorticotropic Hormone** | **2933** | **11.1** | **Glu: 1, Arg: 3, Lys: 4** |
| **Dynorphin A porcine** | **2147** | **11.5** | **Asp: 1, Arg: 3, Lys: 2** |

## 2. Materials and methods

### 2.1. Materials

Recombinant human insulin, human gastrin I, angiotensin I, [$Arg^8$]-vasopressin, luteinizing hormone-releasing hormone (LH-RH), and salmon calcitonin were purchased from Wako Pure Chemical Industries Ltd. (Osaka, Japan). Exendin-4, glucagon-like peptide-1 (GLP-1), leucine enkephalin, oxytocin, thyrotropin-releasing hormone (TRH), leuprolide acetate salt, somatostatin, mastoparan, adrenocorticotropic hormone (ACTH) fragment 1–24, dynorphin A, and biotin were purchased from Sigma-Aldrich Co. (St Louis, MO, USA). D-R8 (rrrrrrrr; r, D-arginine, >90% purity) and biotinylated D-R8 (rrrrrrrrc-biotin; c, D-cysteine, >95% purity) were synthesized by Sigma Genosys, Life Science Division of Sigma-Aldrich Japan Co. (Ishikari, Japan). Carboxymethyl dextran (CM5) and Streptavidin (SA)-coated sensorchips were purchased from GE healthcare UK Ltd. (Buckinghamshire, England). All other chemicals were of analytical grade and are commercially available.

### 2.2. Surface plasmon resonance (SPR)-based binding study

The intermolecular interaction between peptide drugs and CPPs were analyzed by SPR (Biacore 2000, GE healthcare UK).

#### 2.2.1. Binding of peptides to immobilized CPP

To measure the binding of peptides to D-R8, biotinylated-D-R8 was first immobilized to the streptavidin coated on the surface of a SA sensorchip using the strong interaction between biotin and streptavidin. For the immobilization procedure, the biotinylated-D-R8 was diluted to a final concentration of 30 μg/mL using 0.01 M

HEPES buffered solution containing 0.15 M NaCl and 0.005% Surfactant P20 (HBS-P, pH 7.4), (GE healthcare UK) and then immobilized to the surface in separate flow cells at flow rate of 5 μL/min. Biotin (30 μg/mL) was immobilized to the surface of the reference flow cell. For binding measurements, different concentrations of peptide drugs (1–200 μM) were injected for 5 min followed by an additional 5 min dissociation phase. The injections were carried out in HBS-P, pH 6.0 at 20 μL/min and at 25°C. For the experiments using GLP-1, the injections were carried out in HBS-P at pH 6.0 and 7.4 to evaluate the differences arising from pH conditions. At the end of each cycle, the surface was regenerated by 30 s injection of 1 M NaCl.

### 2.2.2. Binding of D-R8 to immobilized insulin

To measure the binding of D-R8 to insulin, insulin was immobilized at the carboxymethyl dextran surface of a CM5 sensorchip using amine coupling. For the immobilization procedure, insulin was diluted to a final concentration of 50 μg/mL using acetate buffer at pH 4.5 and immobilized to the surface in separate flow cells at 10 μL/min for 7 min. The reference surfaces were prepared by amine coupling activation followed by immediate deactivation. For binding measurements, different concentrations of D-R8 (1–100 μM) were injected for 5 min followed by an additional 5 min dissociation phase. At the end of each cycle, the surface was regenerated by 30 s injection of 1 M NaCl. The measurements were carried out in HBS-P, pH 6.0 at 20 μL/min and at 25°C.

### 2.2.3. Analysis of binding characteristics between peptide drugs and D-R

Each sensorgram was shown by subtracting nonspecific binding on the surface of

the reference flow cell from total binding on the peptide drug or D-R8-immobilized surface. Hereinafter, the immobilized molecule is referred to as the 'ligand', and the injected molecule is referred to as the 'analyte'. At first, the equilibrium binding of each cycle was calculated by BIAevaluation software, and then the dissociation constant (KD) and the maximum amount ($R_{max}$) were calculated using equilibrium amounts based on fitting by MULTI software followed by Scatchard analysis. Moreover, the maximum binding capacity at the absorption experimental condition ($B_{max}$) was calculated by using following equation (Eq. 3).

$$B_{max} = [L]_t \cdot R_{max}/L_i \qquad \text{(Eq.3)}$$

where $[L]_t$ is total ligand concentration at absorption experimental condition, and $L_i$ is the amount of immobilized ligand. Furthermore, the bound ($[A]_b$) and unbound ($[A]_f$) analyte concentration at absorption experimental condition were calculated using following equations (Eqs. 4 and 5).

$$[A]_t = [A]_f + B_{max} \cdot [A]_f / (KD + [A]_f) \qquad \text{(Eq.4)}$$

$$[A]_b = [A]_t - [A]_f \qquad \text{(Eq.5)}$$

where $[A]_t$ is total analyte concentration. The bound analyte concentration at absorption experimental condition $[A]_b$ was used as index of binding affinity between peptide drugs and CPPs.

### 2.3. Preparation of drug and D-R8 solution

The specific amounts of peptide drugs or D-R8 were dissolved in phosphate-buffered saline (PBS, pH 6.0 or 7.4) containing 0.001% methylcellulose, which prevents the adsorption of peptide drugs on the tube surface. For preparing the insulin solution, the specific amounts of recombinant human insulin were dissolved in 50 μL of 0.1 M HCl. The insulin solution was diluted to 2.4 mL of PBS (pH 6.0) containing 0.001% methylcellulose, and normalized with 50 μL of 0.1 M NaOH. The peptide drug solution and D-R8 solution were gently mixed to be adjusted to specific concentration. Each drug-D-R8 mixed solution was clear.

### 2.4. In situ loop absorption study

This research was performed at Hoshi University and complied with the regulations of the Committee on Ethics in the Care and Use of Laboratory Animals, and was performed in the same procedures as described in Chapter 1. After the surgical process, 0.5 mL of drug-D-R8 mixed solution or pure drug solution (control) was directly administered into the 6 cm ileal loop made from the 10 cm pretreated segment. The dose of all peptide drugs was adjusted to 331.1 nmol/kg body weight (132 μM). For evaluating the effect of D-R8 on the intestinal absorption of peptide drugs, the dose of D-R8 was 2.5 μmol/kg body weight (1000 μM). For evaluating the dose dependency of D-R8 on insulin-absorption enhancement, the dose of D-R8 was variable from 0.125 to 6.55 μmol/kg body weight (50 to 2620 μM). The pH of drug-D-R8 mixed solution or pure drug solution (control) was adjusted to 6.0. For the experiments using GLP-1, the pH of GLP-1-D-R8 mixed solution or pure GLP-1 solution (control) was adjusted to 6.0 and 7.4 to evaluate the differences arising from different pH conditions.

During the experiments, a 0.25 mL blood aliquot was taken from the jugular vein before and at 5, 10, 15, 30, 60, 120, 180, and 240 min after dosing. Tuberculin syringes (1 mL) were preheparinized in the usual fashion by coating the syringe wall with aspirating heparin and then expelling all heparin by depressing the plunger to the needle hub. Plasma was separated by centrifugation at 13,000 rpm (13,400 × *g*) for 1 min. The plasma concentration of peptide drugs was determined using enzyme immunoassay (EIA) method. An insulin assay kit (Invitron Ltd., Wales, UK), rat GLP-1 ELISA kit (Wako Pure Chemical Industries Ltd., Osaka, Japan), Gastrin I (human) EIA kit, Exendin-4 EIA kit, and Calcitonin (salmon) EIA kit (Phoenix Pharmaceuticals Inc., Burlingame, CA, USA) were used in the experiments. The AUC from 0–4 h was estimated in the same calculations as described in Chapter 1.

**2.5. Statistical analysis**

Each value is expressed as the mean ± standard error (S.E.) of 3–5 determinations. The significance of differences in the mean values was evaluated using Student's unpaired *t* test. For multiple comparisons to evaluate the relationship between D-R8 concentration which bound to insulin and enhancing efficiency of D-R8 on the insulin absorption, analysis of variance (ANOVA) with Dunnett's test was applied. Differences were considered significant when the *p* value was less than 0.05.

## 3. Results

### 3.1. Determination of the binding characteristics between peptide drugs and D-R8

First, the binding of various peptide drugs with different isoelectric points to immobilized D-R8 was measured using an SPR-based method. Figure 13 A and B show the sensorgrams obtained in the binding experiments using gastrin or insulin at pH 6.0. The sensorgram responses increased depending on the injected concentration of these peptides, therefore, these peptides could be considered to bind to D-R8. In contrast, as shown in Fig. 13 C and D, the sensorgram responses did not increase when exendin-4 or calcitonin were injected. Furthermore, like exendin-4 or calcitonin, all other peptides tested would not bind to D-R8 (data not shown). Based on the above-mentioned results, the binding characteristics between gastrin and insulin and D-R8 were analyzed using Scatchard plots (Fig. 14 A and D, and B and E, respectively), and the calculated binding parameters are shown in Table 16. Because the Scatchard plots derived from binding experiments showed two phase-binding patterns as shown in Fig 14 D and E, KD and $R_{max}$ for both phases were calculated and categorized as high- and low-affinity phases. By using these values, the bound concentrations of gastrin and insulin in ileal absorption experiments (the concentrations of these peptides and D-R8 are 132 μM and 1000 μM, respectively) were calculated. As a result of the binding analysis, it was suggested that the bound gastrin and insulin concentrations were 78.4 μM and 77.5 μM (59.4% and 58.7% of total concentration), respectively, and that a large portion of these peptides existed as D-R8 bound form in ileal absorption experiments.

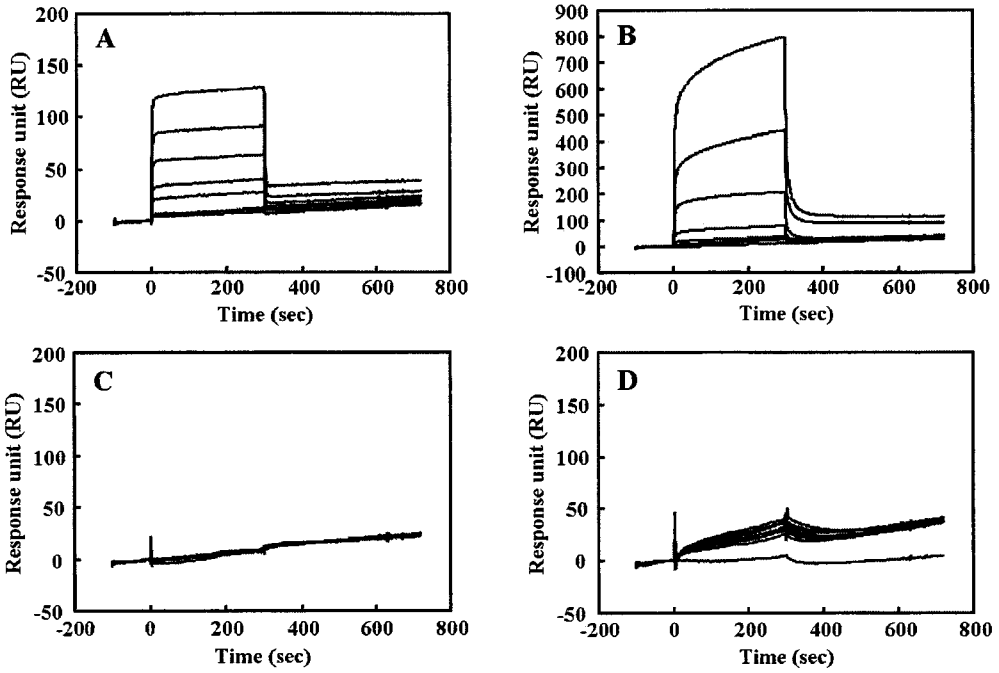


Fig. 13. Binding sensorgrams after injection of various concentrations of peptide drugs into a D-R8-immobilized flow cell at pH 6.0. A: gastrin (1–200 μM). B: insulin (1–200 μM). C: exendin-4 (1–50 μM). D: calcitonin (1–200 μM).

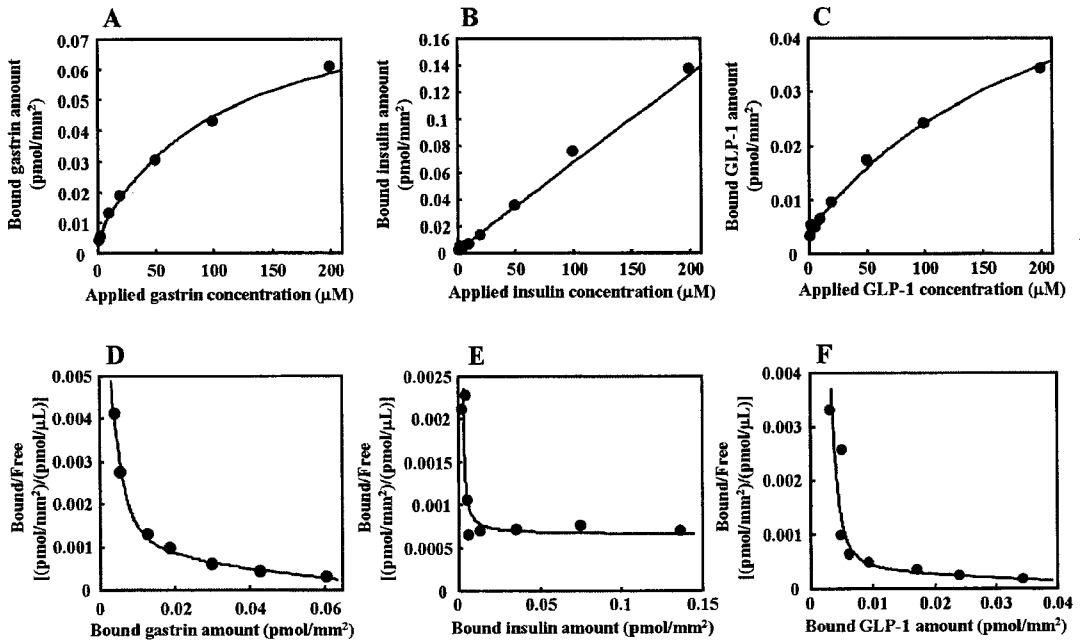


Fig. 14. Binding curves (A, B and C) and Scatchard plots (D, E and F) derived from the binding between gastrin (pH 6.0) (A and D), insulin (pH 6.0) (B and E) or GLP-1 (pH 7.4) (C and F) and immobilized D-R8. Closed circles: experimental data, solid lines: theoretical data obtained by MULTI fitting.

Table 16. Binding parameters between peptide drugs and immobilized D-R8 derived from the SPR study

| | Gastrin (pH6.0) | | Insulin (pH6.0) | | GLP-1 (pH7.4) | |
|---|---|---|---|---|---|---|
| | High | Low | High | Low | High | Low |
| *Binding parameters* | | | | | | |
| Immobilized D-R8 (pmol/mm$^2$) | 0.414 | 0.414 | 0.485 | 0.485 | 0.449 | 0.449 |
| KD (μM) | 0.865 | 112 | $2.95 \times 10^{-2}$ | $9.50 \times 10^{6}$ | 0.328 | 238 |
| Rmax (RU) | 12.8 | 172 | 12.2 | $3.59 \times 10^{7}$ | 13.9 | 222 |
| Rmax (pmol/mm$^2$) | $6.09 \times 10^{-3}$ | $8.21 \times 10^{-2}$ | $2.11 \times 10^{-3}$ | $6.18 \times 10^{3}$ | $4.22 \times 10^{-3}$ | $6.73 \times 10^{-2}$ |
| Binding ratio (Peptide/D-R8) | $1.47 \times 10^{-2}$ | 0.198 | $4.35 \times 10^{-3}$ | $1.28 \times 10^{4}$ | $9.41 \times 10^{-3}$ | 0.150 |
| *In situ absorption experimental condition* | | | | | | |
| Applied peptide (μM) | 132 | | 132 | | 132 | |
| Applied D-R8 (μM) | 1000 | | 1000 | | 1000 | |
| Bmax (μM) | 14.7 | 198 | 4.35 | $1.28 \times 10^{7}$ | 9.41 | 150 |
| Unbound peptide (μM) | 53.6 | | 54.5 | | 83.7 | |
| Bound peptide (μM) | 78.4 | | 77.5 | | 48.3 | |
| Bound peptide ratio (%) | 59.4 | | 58.7 | | 36.6 | |

KD (μM) and Rmax (pmol/mm$^2$) values were calculated from the Scatchard plots depicted in Fig. 14. Binding ratio (Peptide/D-R8) was calculated by dividing Rmax by immobilized D-R8 amount. The parameters at the in situ absorption experimental condition were calculated using equations 3, 4 and 5 described in the Materials and methods section.

### 3.2. Effect of D-R8 on the ileal absorption of peptide drugs

In order to analyze the relationship between the absorption enhancement effect of D-R8 and the binding characteristics between peptide drugs and D-R8, I administered gastrin, insulin, exendin-4, or calcitonin into rat ileal loops in the absence or presence of D-R8. Figure 15 A and B show the effect of D-R8 on the ileal gastrin and insulin absorption, respectively. No apparent absorption was observed following administration of gastrin or insulin solution in the absence of D-R8. In contrast, coadministration of D-R8 significantly increased intestinal gastrin or insulin absorption. Figure 15 C and D show the effect of D-R8 on the ileal exendin-4 and calcitonin absorption, respectively. Unlike for gastrin and insulin, the absorption of exendin-4 and calcitonin were not affected by coadministration of D-R8. Table 17 shows the AUC derived from the plasma

concentration of each peptide–time profile, and indicates that the AUCs of only gastrin and insulin among the four peptides were augmented by coadministration of D-R8.

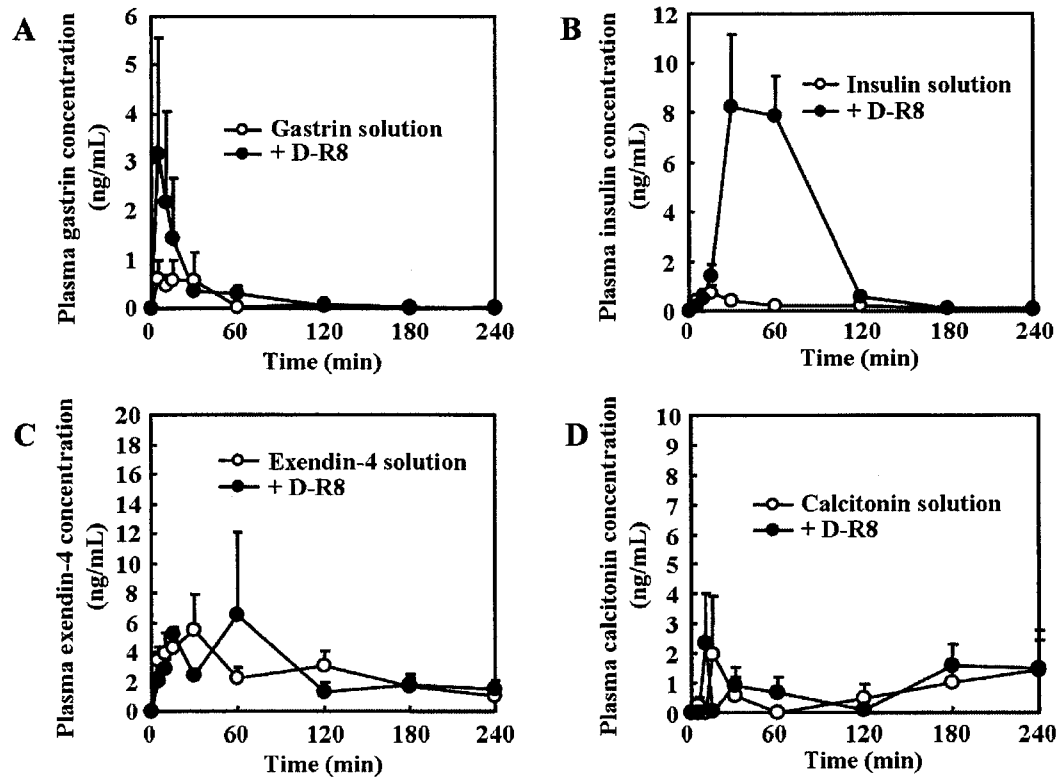


Fig. 15. Plasma peptide-drug concentration vs. time profiles following in situ administration of peptide drugs (132 μM) with D-R8 (1000 μM) into ileal segments at pH 6.0. A: gastrin. B: insulin. C: exendin-4. D: calcitonin. Each data point represents the mean ± S.E. (n = 3–5).

Table 17. AUC following in situ administration of peptide drugs with D-R8 into ileal segments

| | Control (ng·h/mL) | + D-R8 (1000 μM) (ng·h/mL) |
|---|---|---|
| **Gastrin** | **0.55 ± 0.35** | **1.11 ± 0.47** |
| **Insulin** | **0.88 ± 0.32** | **10.02 ± 1.98*** |
| **Exendin-4** | **10.37 ± 2.70** | **10.89 ± 3.12** |
| **Calcitonin** | **2.78 ± 0.79** | **3.48 ± 0.99** |

Each value represents the mean ± S.E. (n = 3–5).
*$p<0.05$, significant difference compared with the corresponding "control".

### 3.3. Determination of the binding characteristics between GLP-1 and D-R8 at different pHs

The binding characteristics between GLP-1 and immobilized D-R8 were examined at different pHs using an SPR-based method. Figure 16 A shows the sensorgrams when various concentrations of GLP-1 were injected into a D-R8-immobilized flow cell at pH 6.0. No apparent increases in sensorgram response were observed at pH 6.0. In contrast, as shown in Fig. 16 B, the sensorgram responses increased depending on the injected concentration of GLP-1 at pH 7.4. In addition, the binding characteristics between GLP-1 and D-R8 at both pHs were analyzed using Scatchard plots (Fig. 14 C and F), and the calculated binding parameters are shown in Table 16. The Scatchard plots derived from experiments using GLP-1 showed two phase-binding patterns as well as the above-mentioned results using gastrin and insulin as shown in Fig. 14 F, so that KD and $R_{max}$ for both phases were calculated and categorized as high- and low-affinity phases. When these binding parameters are applied to absorption experiments (concentrations of GLP-1 and D-R8 were 132 μM and 1000 μM, respectively), the bound concentration of GLP-1 was 48.3 μM (36.6% of total concentration).

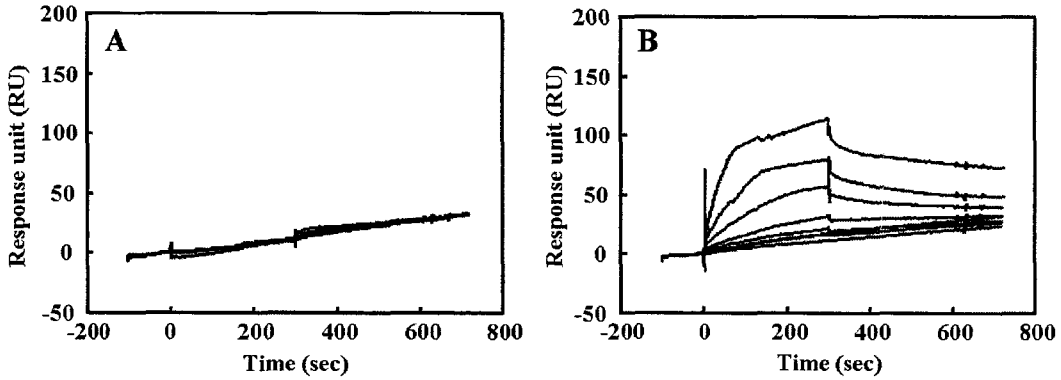


Fig. 16. Binding sensorgrams after injection of various concentrations of GLP-1 into an D-R8-immobilized flow cell. A: pH 6.0 (1–50 μM). B: pH 7.4 (1–200 μM).

### 3.4. Effect of D-R8 on the ileal GLP-1 absorption at different pHs

Figure 17 A and B show the effect of D-R8 on the ileal GLP-1 absorption following administration at pH 6.0 and 7.4, respectively. In both cases, the absorption of GLP-1 was elevated by coadministration of D-R8 with GLP-1. Figure 17 C shows the AUC derived from the plasma GLP-1 concentration–time profile. The increase of AUC by coadministration of D-R8 at pH 6.0 was approximately 2.69 fold. In contrast, the increase of AUC by coadministration of D-R8 at pH 7.4 was approximately 6.86 fold.

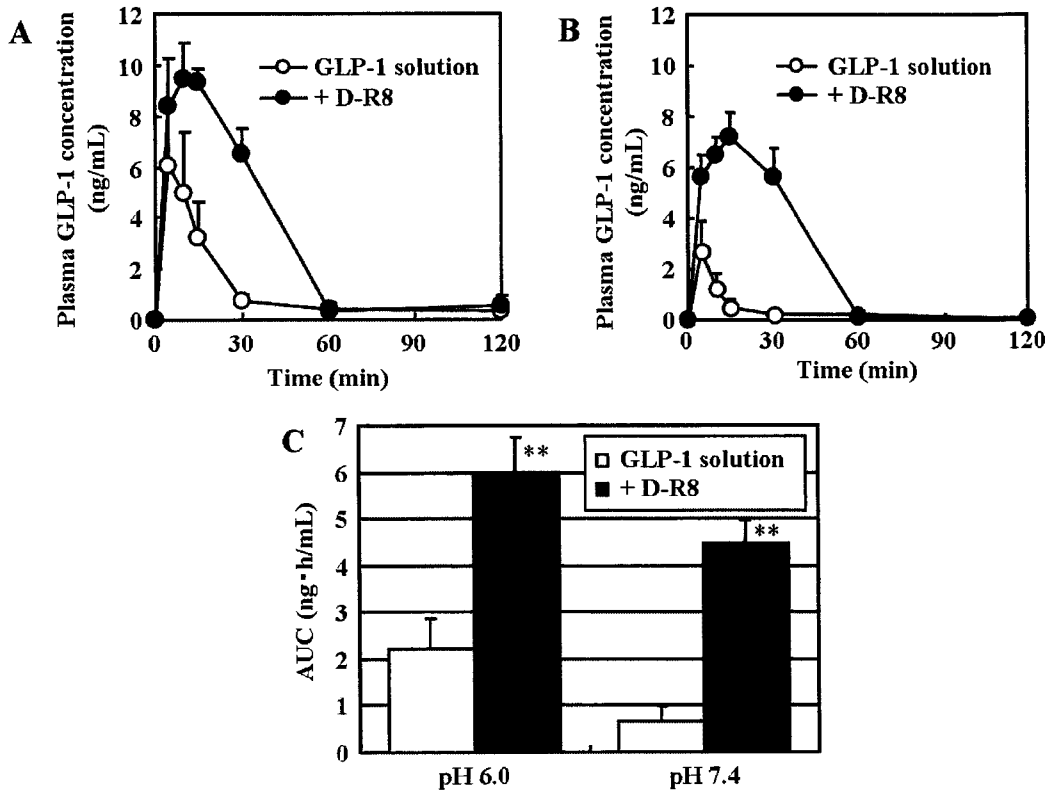


Fig. 17. Plasma GLP-1 concentration vs. time profiles (A: pH 6.0; B: pH 7.4) and AUC of GLP-1 (C) following in situ administration of GLP-1 (132 μM) with D-R8 (1000 μM) into ileal segments. Each value represents the mean ± S.E. (n = 3–4). $^{**}p<0.01$, significant difference compared with the corresponding "GLP-1 solution".

### 3.5. Relationship between applied and bound D-R8 concentrations

To calculate the concentration of D-R8 bound to insulin when D-R8 was applied at various doses in absorption experiments, the binding characteristics between D-R8 and immobilized insulin were analyzed using an SPR-based method. Figure 18 A shows the sensorgrams when various concentrations of D-R8 were injected into an insulin-immobilized flow cell at pH 6.0. The sensorgram responses increased depending on the injected concentration of D-R8 as well as the when insulin solutions were inversely injected into a D-R8-immobilized flow cell as shown in Fig. 13 B. In addition, the binding characteristics between D-R8 and insulin were analyzed using Scatchard plots (Fig. 18 B and C), and the calculated binding parameters are shown in Table 18. The Scatchard plots derived from these experiments showed a two phase-binding pattern as shown in Fig. 18 C, so that KD and $R_{max}$ for both phases were calculated and categorized as high- and low-affinity phases. Moreover, the concentrations of bound D-R8, when D-R8 was added at various concentrations to 132 μM of insulin solution in the absorption experiments, were calculated. As shown in Fig. 19, the bound D-R8 concentration was augmented depending on the increase of total D-R8 concentration added to insulin solution.

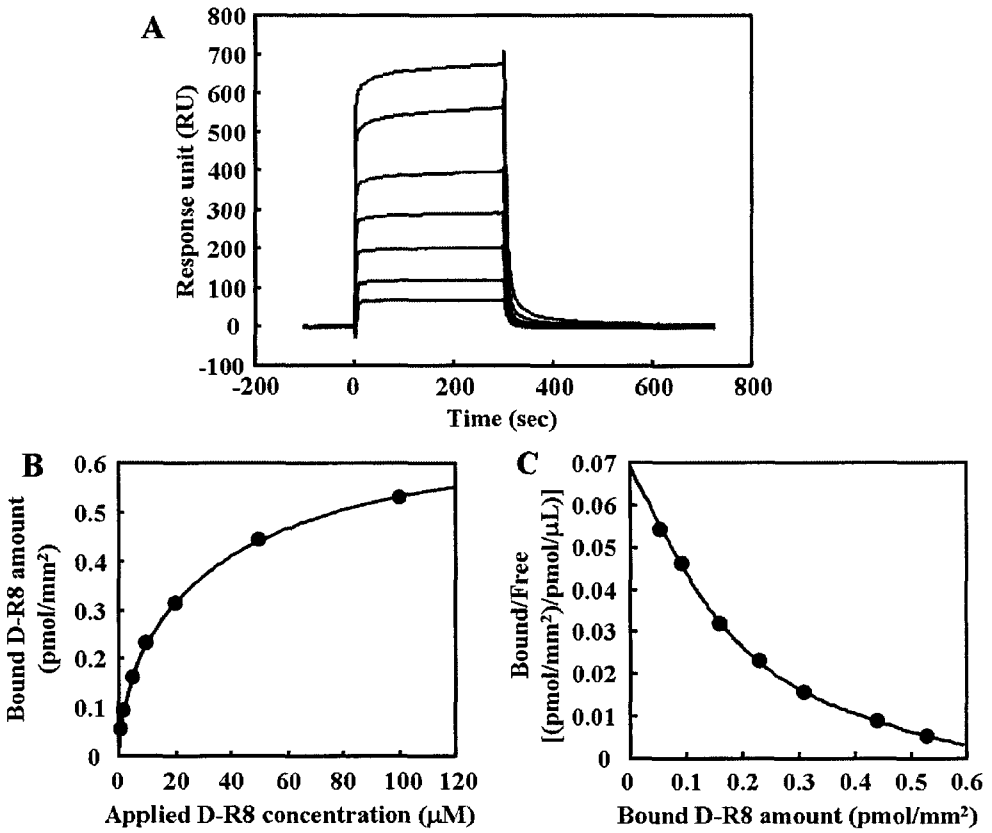


Fig. 18. Binding sensorgrams after injection of various concentrations (1–100 μM) of D-R8 into an insulin-immobilized flow cell at pH 6.0 (A), and the binding curve (B) and Scatchard plot (C) derived from the binding between D-R8 and immobilized insulin (pH6.0). Closed circles: experimental data, solid lines: theoretical data obtained by MULTI fitting.

Table 18. Binding characteristics between D-R8 and immobilized insulin derived from the SPR study at pH 6.0

| | D-R8 | |
|---|---|---|
| | **High** | **Low** |
| **Immobilized insulin amount (pmol/mm²)** | **0.269** | **0.269** |
| **KD (μM)** | **3.01** | **44.8** |
| **Rmax (RU)** | **219** | **667** |
| **Rmax (pmol/mm²)** | **0.173** | **0.526** |
| **Binding ratio (D-R8/insulin)** | **0.641** | **1.96** |

KD (μM) and $R_{max}$ (pmol/mm$^2$) values were calculated from the Scatchard plots depicted in Fig. 18, and the binding ratio (D-R8/insulin) was calculated by dividing Rmax by immobilized insulin amount.

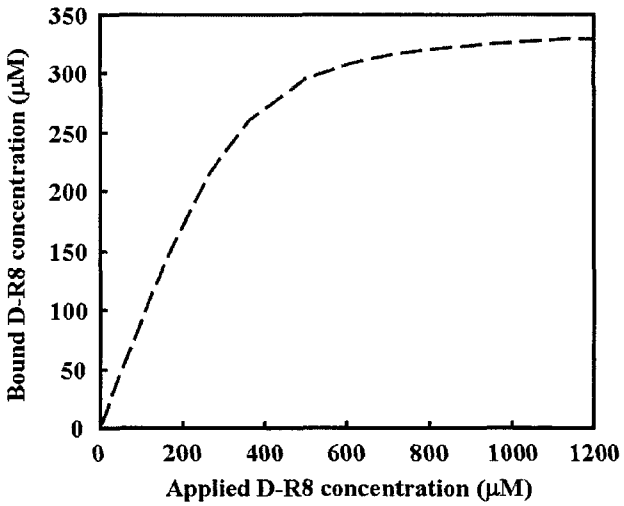


Fig. 19. Relationship between the total D-R8 concentration added to the insulin solution (132 μM) and the D-R8 concentration bound to insulin. The D-R8 concentration bound to insulin were calculated using parameters described in Table 18 and equations 3, 4 and 5 described in the Materials and methods section.

### 3.6. Relationship between bound D-R8 concentration and absorption-enhancing efficiency of D-R8

To determine the relationship between the bound D-R8 concentration and the increased efficiency of ileal insulin absorption using D-R8, insulin was coadministered with various concentrations of D-R8. Figure 20 A shows the time profiles of plasma insulin concentrations following the ileal administration of insulin with various concentrations of D-R8. The insulin absorption was elevated depending on the coadministered D-R8 concentration. Each concentration of coadministered D-R8 was converted to the concentration bound to insulin based on Fig. 19, and then the AUC derived from the plasma insulin concentration–time profile was stated in relation to the bound D-R8 concentration in Fig. 20 B. The AUC was not augmented at concentrations less than approximately 200 μM of bound D-R8. When the bound D-R8 concentration was approximately 250 μM, the AUC was linearly augmented.

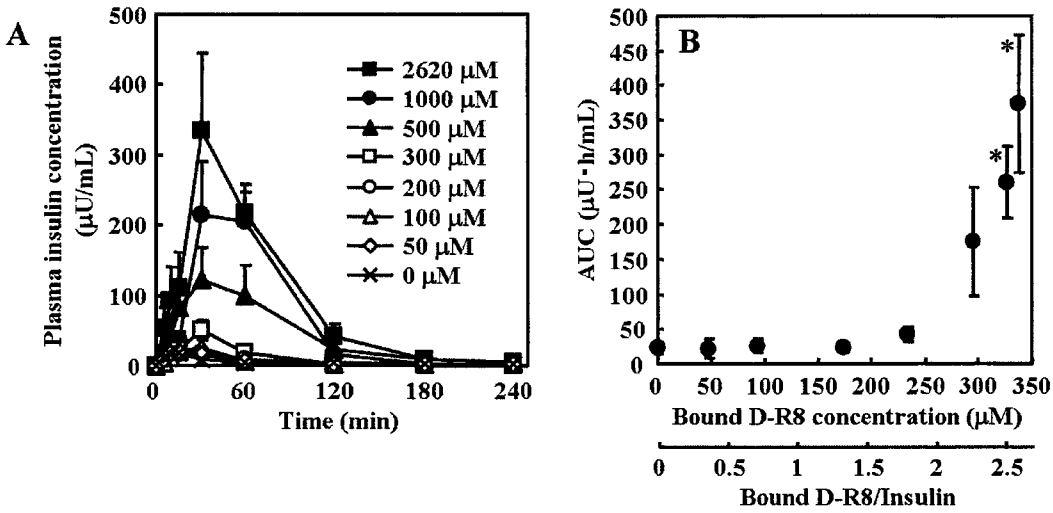


Fig. 20. Plasma insulin concentration vs. time profiles following in situ administration of insulin (132 μM) with various concentrations of D-R8 into ileal segments (A) and the relationship between bound D-R8 concentration and enhancing efficiency of insulin absorption by D-R8 (B). Each value represents the mean ± S.E. (n = 3–5). *$p$<0.05, significant difference compared with the corresponding "0 μM of D-R8".

## 4. Discussion

My approach using CPPs has achieved significant improvement in intestinal absorption by coadministration of therapeutic peptides and proteins and CPPs as a physical mixture, as distinct from the conventional method of using CPPs for intracellular delivery in which CPPs are covalently linked to drugs and carriers. The pharmacological activity of therapeutic peptides and proteins may be lost by CPP conjugation, and the absorption of leuprolide-D-R6 conjugate was not found to be higher than leuprolide itself as shown in Chapter 3. Therefore, the conjugation approach may not favorable for absorption into circulation. In contrast, I have demonstrated that my approach using a physical mixture does not have such disadvantages and shows sufficient pharmacological effect as shown in Chapters 1 and 2. It has been demonstrated that the ability of a CPP to enhance intestinal drug absorption is different depending on the kind of drug. Based on the physical properties of drugs, it had been proposed that the electrostatic interaction between each drug and a positively charged CPP may be associated with the absorption-enhancing efficiency of CPP coadministration. However, until now there was no evidence for this link. Therefore, the present study aimed to elucidate the characteristics of the binding between macromolecular drugs and CPPs and to establish their relationship with the absorption-enhancing effect of CPP coadministration.

First, various peptide drugs with different isoelectric points, as shown in Table 15, were used, and the binding characteristics between the drugs and D-R8 and the effect of coadministration of D-R8 on drug intestinal absorption were examined. As shown in Fig. 13 A and B, the sensorgram response increased depending on injected peptide concentration after gastrin or insulin was injected into a D-R8-immobilized flow cell at

pH 6.0. In contrast, no increase of the sensorgram response was observed after other peptide drugs including exendin-4 and calcitonin were injected (Fig. 3 C and D, data for other peptides is not shown). Because gastrin and insulin have low isoelectric points (Table 15), they are negatively charged at pH 6.0, and so it is proposed that their binding to positively charged D-R8 was observed. In contrast, most peptide drugs that cannot bind to D-R8 have high isoelectric points and are positively charged at pH 6.0. Therefore, it is suggested that no binding was observed between these peptide drugs and D-R8. However, exendin-4, oxytocin, and a few peptides cannot bind to D-R8 at this pH despite their low isoelectric points. It is proposed that factors other than electrostatic characteristics, such as hydrophobicity and tertiary structure, may be associated with intermolecular interactions between peptide drugs and D-R8. Subsequently, Scatchard analysis of the binding characteristics between gastrin and insulin and D-R8 demonstrated that the bound concentrations of gastrin and insulin in an in situ loop absorption experiment (mixture of 132 μM peptide drug and 1000 μM D-R8) were 59.4% and 58.7%, respectively (Table 16). Later, the effect of coadministration of D-R8 on the intestinal absorption of these peptide drugs was examined in an in situ loop absorption study. In this study, gastrin and insulin were used as peptide drugs that bind to D-R8, and exendin-4 and calcitonin were used as peptide drugs that do not bind to D-R8. As shown in Fig. 15 A and B and Table 17, the absorption of gastrin and insulin increased in the presence of D-R8. In contrast, as shown in Fig. 15 C and D and Table 17, the absorption of exendin-4 and calcitonin was not affected by coadministration of D-R8. Based on these results, the absorption-enhancing effect of coadministration of drugs and D-R8 corresponds with intermolecular binding between the drug and D-R8, implying that this binding is an important factor governing the enhancing effect of D-R8

on the intestinal absorption of macromolecular drugs.

To elucidate this involvement, the absorption-enhancing effect of D-R8 at different binding conditions was examined by altering the pH conditions. In this study, GLP-1 was used as a model peptide drug. As shown in Fig. 16 A, no increase of sensorgram response was observed after injection of GLP-1 into a D-R8-immobilized flow cell at pH 6.0. In contrast, as shown in Fig. 16 B, the sensorgram response increased depending on the injected GLP-1 concentration after injection of GLP-1 at pH 7.4. It is speculated that charge disposition of GLP-1 weakened at pH 6.0, because the pH was close to its isoelectric point. In contrast, GLP-1 tended to possess negative charge at pH 7.4. Therefore, I speculate that the change in charge disposition contributed to variation in the binding characteristics depending on the pH of the environment. Moreover, an analysis of the binding parameters between GLP-1 and D-R8 at pH 7.4 demonstrated that the bound concentration of GLP-1 in an in situ loop experiment (mixture of 132 μM GLP-1 and 1000 μM D-R8) was 36.6% (Table 16). Later, in situ loop absorption experiments were conducted using a physical mixture of GLP-1 and D-R8 prepared at pH 6.0 or 7.4. As shown in Fig. 17 C, the increases in the AUC after administration at pH 6.0 and 7.4 were 2.69 and 6.86 fold, respectively. Thus, a stronger enhancing effect on intestinal GLP-1 absorption was observed after administration at pH 7.4, at which GLP-1 can strongly bind to D-R8. I propose that the increase of GLP-1 absorption after administration at pH 6.0, at which GLP-1 cannot bind to D-R8, was because of a gradual increase of pH in the mixture followed by the formation of a complex, as the pH of the ileal lumen is intrinsically neutral. Thus, both the binding efficiency between GLP-1 and D-R8 and the enhancement of intestinal GLP-1 absorption were affected by altering the pH of mixture, suggesting that the

binding characteristics between the drug and D-R8 were associated with the enhancement of intestinal absorption by D-R8.

Furthermore, the relationship between the concentration of D-R8 that bound to the peptide drug in an in situ loop absorption experiment and the absorption-enhancing efficiency of D-R8 were evaluated. In this evaluation, insulin was used as model peptide drug. To estimate the change in bound D-R8 concentration by altering the concentration of D-R8 added to insulin, the binding characteristics between D-R8 and immobilized insulin at pH 6.0 were measured. As shown in Fig. 18 A, the sensorgram response increased depending on the concentration of injected D-R8 in the above-mentioned experiment in which insulin was injected into a D-R8-immobilized- flow cell (Fig. 13 B). Based on this result, the concentration of D-R8 that bound to insulin in an in situ loop absorption experiment when various concentrations of D-R8 were mixed with insulin was estimated by calculating the binding parameters between D-R8 and immobilized insulin (Table 18). As shown in Fig. 19, the concentration of D-R8 that bound to insulin increased following an increase in the D-R8 concentration, but tended to saturate at approximately 350 μM. Subsequently, physical mixtures of insulin and various concentrations of D-R8 were administered. As shown in Fig. 20 A, augmentation of intestinal insulin absorption was observed following an increase of mixed D-R8 concentration. Here, to elucidate the relationship between the AUC of insulin and bound D-R8 concentration, each concentration of mixed D-R8 was converted to the bound D-R8 concentration, based on the result shown in Fig. 19 (Fig. 20 B). It was found that the AUC of insulin was not affected in the presence of a bound D-R8 concentration lower than approximately 250 μM. In contrast, the AUC of insulin linearly increased when the bound D-R8 concentration was more than approximately 250 μM. Under these

conditions of D-R8–insulin binding, it was noted that the binding ratio between insulin and D-R8 was approximately 1:2. Therefore, I suggest that the binding of two D-R8 molecules to one insulin molecule is needed to enhance intestinal insulin absorption by the coadministration of D-R8. Thus, the binding ratio between a drug and CPP obtained in binding experiments may be an index by which to estimate the dose of CPP needed to enhance intestinal absorption. However, the further study may be needed to identify the accurate binding ratio required to enhance the intestinal insulin absorption, because the bound D-R8 concentration determined on the SPR-based binding assay may not completely reflect the interaction behavior in bulk solution due to restricted movement of insulin by its immobilization on the flow cell.

The study presented in this chapter demonstrated the importance of intermolecular binding between drug and CPP in the strategy of using CPPs to enhance the intestinal absorption of macromolecular drugs. The findings in this study suggest peptides and proteins whose absorption is possibly improved by coadministration of CPPs may be screened by measuring the intermolecular binding between drug and CPP, and it is expected that the optimal use of CPPs as a tool for the intestinal delivery of therapeutic peptides and proteins will be attained. On the other hand, although D-R8 was used as model CPP in this study, CPPs have wide diversity and include arginine-rich and amphipathic peptides. Therefore, I propose that the binding between a drug and a CPP, such as electrostatic and hydrophobic interactions and hydrogen bonding, is different depending on the type of CPP. The measuring of binding characteristics between a drug and various CPPs is needed to determine which CPPs would most effectively enhance intestinal absorption. In addition, although it was demonstrated that the intermolecular binding between a drug and CPP is an important factor in

intestinal-absorption enhancement, the mechanisms for the uptake of a complex by epithelial cells and its subsequent release to circulation are not clear. In Chapter 3, I demonstrated that the absorption of a fusogenic peptide consisting of leuprolide and D-R6, an oligoarginine, was lower than that of leuprolide alone. Therefore, it is difficult for a drug–CPP complex formed via an electrostatic interaction to circulate as an intact complex. Moreover, in my study using isolated rat ileal membrane shown in Chapter 3, it was proven that the uptake of D-R6 by ileal epithelial membrane is mediated by the electrostatic adsorption of D-R6 onto cell-surface proteoglycans as the initial process. It is possible that a drug–CPP complex is dissociated on the cell surface by competitive interaction between CPP and proteoglycans. In addition, my study shown in Chapter 3 demonstrated that D-R6 adsorbed by proteoglycans was internalized into ileal epithelium via an energy-dependent pathway, so the complex may be dissociated in acidic compartments, such as endosomes, after it is taken up by epithelial cells. Furthermore, not only the binding efficiency between a drug and CPP but also other factors such as the internalization efficiency of the CPP itself may affect intestinal-absorption enhancement. Thus, although further examination is essential for understanding the complete mechanisms for the absorption-enhancing effect of CPPs, to the best of my knowledge the study presented here is the first reported evidence for a relationship between intermolecular binding of peptide or protein drugs and CPPs and the enhancing effect of CPP coadministration on their intestinal absorption. Therefore, this study may provide information for the development of successful oral delivery systems for therapeutic peptides and proteins using CPPs.

## 5. Conclusions

The study presented here was conducted to determine the importance of intermolecular binding between macromolecular drugs and CPPs on the improvement of the intestinal macromolecular drug absorption using CPPs. I have demonstrated that coadministration with D-R8 can enhance the intestinal absorption only of peptides that are able to bind to D-R8. In addition, I have demonstrated that the binding ratio between insulin and D-R8 is an important factor in enhancing intestinal insulin absorption by coadministration of D-R8. Thus, the intermolecular interaction between drugs and CPPs is related to the efficiency of the absorption-enhancing effect of CPPs on intestinal macromolecular drug absorption.

# SUMMARY

During the past few decades, the biotherapeutic agents such as peptides and proteins have been contributed to the treatment of several diseases. However, their oral absorption is significantly limited due to the presence of significant barriers in gastrointestinal tract, such as enzymatic degradation and mucosal membrane. Therefore, the feasible approaches are needed for developing the oral forms of therapeutic peptides and proteins.

Meanwhile, recent reports indicated that cell-penetrating peptides (CPPs) such as HIV-1 Tat and oligoarginine are considered as a useful tool for the intracellular delivery of therapeutic macromolecules. Hence, it was expected that the ability of CPPs may be applicable to enhance the absorption of therapeutic peptides and proteins through intestinal epithelial membrane. One study suggested that the permeation of insulin through Caco-2 cell monolayer, which is one of in vitro model intestinal membranes, was enhanced by crosslinking with HIV-1 Tat peptide [49]. However, there is no information about improvement of intestinal macromolecular drug absorption using CPPs on the biological membrane.

In this thesis, the approach based on physical mixture of macromolecular drugs and CPPs was attempted to actually realize the sufficient intestinal absorption of therapeutic peptides and proteins. Furthermore, the mechanisms associated with absorption enhancing effect of CPPs on the intestinal absorption of these drugs were studied.

At first, the study presented in Chapter 1 aimed to evaluate whether oligoarginine, typical CPP, can improve intestinal absorption of insulin in rats. Intestinal insulin

absorption increased dramatically after coadministration of arginine-hexamer (R6) in a dose-dependent manner, and the effects on insulin absorption were more pronounced for D-R6 than for L-R6. Among oligoarginines composed of six, eight, or 10 arginine residues, D-R8 showed the strongest enhancing effects on insulin intestinal absorption. In contrast, intestinal absorption of other model hydrophilic macromolecules, IFN-β and FD-4, were not affected by coadministration with oligoarginine. Furthermore, oligoarginine has no untoward effect on the intestinal mucosa. The results shown in Chapter 1 demonstrate that coadministration of oligoarginine with insulin is more convenient and safer approach to improve its intestinal absorption without causing detectable damage in cellular integrity.

The study presented in Chapter 2 aimed to identify CPPs that are more effective for the delivery of insulin and do not induce toxic effects on the intestine. In this study, I examined the effects of various types of CPPs including arginine-rich peptides and amphipathic peptides that aid insulin absorption from rat ileal segments. Among these peptides, L-penetratin had the strongest ability to enhance intestinal insulin absorption. Meanwhile, in a physical mixture of CPP and insulin, aggregates formed in the solution when high concentrations CPPs were present. L-penetratin enhanced insulin absorption even when administered in an aggregated solution. I then showed that aggregates of L-penetratin and insulin were broken down in the presence of intestinal degradation enzymes. Thus, among CPPs used in this study, L-penetratin had the strongest ability to improve insulin intestinal absorption.

In Chapter 3, the permeation characteristics of oligoarginine itself across the intestinal membrane were determined to obtain the information about absorption enhancement mechanisms. Incubation at low temperature and coincubation with heparin

reduced the tissue distribution and permeation of FL-D-R6 through the rat ileal membrane. These results suggest that the attachment of FL-D-R6 to cell-surface proteoglycans and energy-dependent endocytosis are involved in its permeation through the ileal epithelial membrane. Based on the characteristics of oligoarginine, I attempted to facilitate the intestinal permeation of the peptide drug, leuprolide, using the function of oligoarginine. However, leuprolide permeation was not achieved when leuprolide was applied with oligoarginine to mucosal side of rat ileal sheets or when a leuprolide–oligoarginine conjugate was administered. These findings emphasize that any strategy using oligoarginine to improve intestinal drug permeation requires an intermolecular interaction, such as an electrostatic interaction, and a covalent linkage between the macromolecular drug and oligoarginine may hamper the ability of oligoarginine to enhance intestinal epithelial permeation of therapeutic peptides and proteins.

In Chapter 4, I verified the hypothesis that the electrostatic interaction between drug and CPP is related to the enhancing effect of the CPP on the intestinal absorption of therapeutic peptides and proteins. Among the 16 peptide drugs possessing different isoelectric points, it was observed that only gastrin, insulin and GLP-1 bound to D-R8, and subsequently their intestinal absorption increased by coadministration of D-R8. In contrast, the intestinal absorption of other peptide drugs that did not bind to D-R8 was not affected in the presence of D-R8. Furthermore, as the results of Scatchard analysis showed, D-R8 increased intestinal insulin absorption when two D-R8 molecules were bound to an insulin molecule. This study suggests that intermolecular binding between drug and CPP is an important factor governing the enhancing effect of the CPP on the intestinal absorption of therapeutic peptides and proteins.

In conclusion, CPPs are likely to become powerful tools for overcoming the low permeability of therapeutic peptides and proteins through the epithelial cell membrane, the major barrier to their oral delivery. Further advantage of this promising strategy is that this successful intestinal absorption could be achieved by more convenient methodology, coadministration of CPP with drugs via intermolecular interaction among them. Hereafter, the further establishment of delivery system based on CPPs is required to realize the development of the oral forms of therapeutic peptides and proteins.

## ACKNOWLEDGEMENTS

First of all, I would like to express my gratitude and appreciation from my heart to Professor Kozo Takayama and Associate Professor Mariko Morishita for their guidance and advice in my research work and preparing this dissertation.

Secondly, I would like to also express my great appreciation to Dr. Nobuo Ida, Dr. Reiji Nishio (New Frontiers Research Laboratories, Toray Industries, Inc.), Professor Masahiro Goto and Associate Professor Noriho Kamiya (Department of Applied Chemistry, Graduate School of Engineering, Kyushu University) for their helpful guidance and assistance in my research work.

Further, I wish to thank Professor Yuichi Sugiyama (Department of Molecular Pharmacokinetics, Graduate School of Pharmaceutical Sciences, the University of Tokyo) for his valuable suggestions.

Moreover, I would like to thank Dr. Koichi Isowa (Japan Biological Science Inc.) and Professor Noriko Takahashi (Physiological Chemistry Research Laboratory, Institute of Medicinal Chemistry, Hoshi University) for their helpful assistance in my research work.

Also, I wish to thank Dr. Yasuko Obata, Dr. Yoshinori Onuki (Department of Pharmaceutics, Hoshi University), Mr. Jumpei Ehara (Bushu Pharmaceuticals Ltd.), Dr. Koji Nakamura (Terumo Corp.), Dr. Yoshinobu Aoki, Dr. Takahiro Goto (Kyorin

Pharmaceutical Co., Ltd.), Ms. Hitomi Chiba (Kowa Co., Ltd.) and Dr. Tetsuo Yamagata (Merck KGaA) for their valuable suggestions and fruitful discussions.

In addition, I am grateful to Mr. Yu Fukuoka, Mr. El-Sayed Khafagy, Ms. Yoshimi Eda, Mr. Yohei Ikeno, Mr. Yoshiaki Terasawa, Mr. Shuichi Yamamoto, Ms. Emi Ito, Ms. Chie Sugimoto, Mr. Shigeaki Matayoshi, Ms. Hiroko Takagi and all my colleagues of the Department of Pharmaceutics of Hoshi University for their kindness and assistance.

Finally, I wish to express my sincere gratitude to my parents, brother and friends. This thesis would not have been fulfilled without their encouragement and support of my study and life.

# REFERENCES


[1] I.B. Hirsch, Drug Therapy: Insulin Analogues, N. Engl. J. Med. 352 (2005) 174-183.

[2] J.H. Hoofnagle, A.M. Di Bisceglie, Drug Therapy: The Treatment of Chronic Viral Hepatitis, N. Engl. J. Med. 336 (1997) 347-356.

[3] L.T. Goodnough, T.G. Monk, G.L. Andriole, Current Concepts: Erythropoietin Therapy, N. Engl. J. Med. 336 (1997) 933-938.

[4] M. Goldberg, I. Gomez-Orellana, Challenges for the oral delivery of macromolecules, Nat. Rev. Drug Discov. 2 (2003) 289-295.

[5] D.R. Owens, B. Zinman, G. Bolli, Alternative routes of insulin delivery, Diabetic Medicine, 20 (2003) 886-898.

[6] M. Morishita, N.A. Peppas, Is the oral route possible for peptide and protein drug delivery?, Drug Discov. Today, 11 (2006) 905-910.

[7] El-S. Khafagy, M. Morishita, Y. Onuki, K. Takayama, Current challenges in non-invasive insulin delivery systems: A comparative review, Adv. Drug Delliv. Rev. 59 (2007) 1521-1546.

[8] J.F. Woodley, Enzymatic barriers for GI peptide and protein delivery, Crit. Rev. Ther. Drug. Carrier. Syst. 11 (1994) 61-95.

[9] L.L. Chang, J.P.F. Bai, Evidence for the existence of insulin-degrading enzyme on the brush-border membranes of rat enterocytes, Pharm. Res. 13 (1996) 801-803.

[10] M. Morishita, I. Morishita, K. Takayama, Y. Machida, T. Nagai, Site-dependent effect of aprotinin, sodium caprate, $Na_2EDTA$ and sodium glycocholate on intestinal absorption of insulin. Biol. Pharm. Bull. 16 (1993) 68-72.

[11] A. Yamamoto, T. Taniguchi, K. Rikyuu, T. Tsuji, T. Fujita, M. Murakami, S. Muranishi, Effect of various protease inhibitors on the intestinal absorption and degradation of insulin in rats, Pharm. Res. 11 (1994) 1496-1500.

[12] H. Liu, R. Tang, W.S. Pan, Y. Zhang, H. Liu, Potential utility of various protease inhibitors for improving the intestinal absorption of insulin in rats, J. Pharm. Pharmacol. 55 (2003) 1523-1529.

[13] G.P. Carino, J.S. Jacob, E. Mathiowitz, Nanosphere based oral insulin delivery, J. Control. Release 65 (2000) 261-269.

[14] R. Qi, Q.N. Ping, Gastrointestinal absorption enhancement of insulin by administration of enteric microspheres and SNAC to rats, J. Microencapsul. 21 (2004) 37-45.

[15] H. Takeuchi, H. Yamamoto, T. Niwa, T. Hino, Y. Kawashima, Enteral absorption of insulin in rats from mucoadhesive chitosan-coated liposomes, Pharm. Res. 13 (1996) 896-901.

[16] H. Takeuchi, Y. Matsui, H. Yamamoto, Y. Kawashima, Mucoadhesive properties of carbopol or chitosan-coated liposomes and their effectiveness in the oral administration of calcitonin to rats,

J. Control. Release. 86 (2003) 235-242.

[17] Z. Degim, N. Unal, D. Essiz, U. Abbasoglu, The effect of various liposome formulations on insulin penetration across Caco-2 cell monolayer, Life. Sci. 75 (2004) 2819-2827.

[18] A. Matsuzawa, M. Morishita, K. Takayama, T. Nagai, Absorption of insulin using water-in-oil-in-water emulsion from an enteral loop in rats, Biol. Pharm. Bull. 18 (1995) 1718-1723.

[19] M. Morishita, M. Kajita, A. Suzuki, K. Takayama, Y. Chiba, S. Tokiwa, T. Nagai, The dose-related hypoglycemic effects of insulin emulsions incorporating highly purified EPA and DHA, Int. J. Pharm. 201 (2000) 175-185.

[20] A. Lawman, M. Morishita, M. Kajita, T. Nagai, N. Peppas, Oral delivery of insulin using pH-responsive complexation gels, J. Pharm. Sci. 88 (1999) 933-937.

[21] M. Morishita, T. Goto, N.A. Peppas, J.I. Joseph, M.C. Torjman, C. Munsick, K. Nakamura, T. Yamagata, K. Takayama, A.M. Lowman, Mucosal insulin delivery systems based on complexation polymer hydrogels: effect of particle size on insulin enteral absorption, J. Control. Release. 97 (2004) 115-124.

[22] T. Yamagata, M. Morishita, N.J. Kavimandan, K. Nakamura, Y. Fukuoka, K. Takayama, N.A. Peppas, Characterization of insulin protection properties of complexation hydrogels in gastric and intestinal enzyme fluids, J. Control. Release 112 (2006) 343-349.

[23] J.C. Scott-Moncrieff, Z. Shao, A.K. Mitra, Enhancement of intestinal insulin absorption by bile salt-fatty acid mixed micelles in dogs, J. Pharm. Sci. 83 (1994) 1465-1469.

[24] T. Uchiyama, T. Sugiyama, Y.S. Quan, A. Kotani, N. Okada, T. Fujita, S. Muranishi, A. Yamamoto, Enhanced permeability of insulin across the rat intestinal membrane by various absorption enhancers: their intestinal mucosal toxicity and absorption-enhancing mechanism of n-lauryl-beta-D-maltopyranoside, J. Pharm. Pharmacol. 51 (1999) 1241-1250.

[25] S. Futaki, Arginine-rich peptides: potential for intracellular delivery of macromolecules and the mystery of the translocation mechanisms, Int. J. Pharm. 245 (2002) 1-7.

[26] S. Futaki, Membrane-permeable arginine-rich peptides and the translocation mechanisms, Adv. Drug. Deliv. Rev. 57 (2005) 547-558.

[27] S. Futaki, T. Suzuki, W. Ohashi, T. Yagami, S. Tanaka, K. Ueda, Y. Sugiura, Arginine-rich peptides. An abundant source of membrane-permeable peptides having potential as carriers for intracellular protein delivery, J. Biol. Chem. 276 (2001) 5836-5840.

[28] I. Nakase, T. Takeuchi, G. Tanaka, S. Futaki, Methodological and cellular aspects that govern the internalization mechanisms of arginine-rich cell-penetrating peptides, Adv. Drug Deliv. Rev. 60 (2008) 598-607.

[29] E. Vives, P. Brodin, B. Lebleu, A truncated HIV-1 Tat protein basic domain rapidly translocates through the plasma membrane and accumulates in the cell nucleus, J. Biol. Chem. 272 (1997)

16010-16017.

[30] S. Futaki, T. Suzuki, W. Ohashi, T. Yagami, S. Tanaka, K. Ueda, Y. Sugiura, Arginine-rich peptides. An abundant source of membrane-permeable peptides having potential as carriers for intracellular protein delivery, J. Biol. Chem. 276 (2001) 5836-5840.

[31] D.J. Mitchell, D.T. Kim, L. Steinman, C.G. Fathman, J.B. Rothbard, Polyarginine enters cells more efficiently than other polycationic homopolymers, J. Pept. Res. 56 (2000) 318-325.

[32] D. Derossi, A.H. Joliot, G. Chassaing, A. Prochiantz, The third helix of the Antennapedia homeodomain translocates through biological membranes, J. Biol. Chem. 269 (1994) 10444-10450.

[33] J.P. Richard, K. Melikov, E. Vives, C. Ramos, B. Verbeure, M.J. Gait, L.V. Chernomordik, B. Lebleu, Cell-penetrating peptides. A reevaluation of the mechanism of cellular uptake, J. Biol. Chem. 278 (2003) 585-590.

[34] C. Marty, C. Meylan, H. Schott, K. Ballmer-Hofer, R.A. Schwendener, Enhanced heparan sulfate proteoglycan-mediated uptake of cell-penetrating peptide-modified liposomes, Cell. Mol. Life. Sci. 61 (2004) 1785-1794.

[35] M. Tyagi, M. Rusnati, M. Presta, M. Giacca, Internalization of HIV-1 Tat requires cell surface heparan sulfate proteoglycans, J. Biol. Chem. 276 (2001) 3254-3261.

[36] J.S. Wadia, R.V. Stan, S.F. Dowdy, Transducible TAT-HA fusogenic peptide enhances escape of TAT-fusion proteins after lipid raft macropinocytosis, Nat. Med. 10 (2004) 310-315.

[37] I. Nakase, M. Niwa, T. Takeuchi, K. Sonomura, N. Kawabata, Y. Koike, M. Takehashi, S. Tanaka, K. Ueda, J.C. Simpson, A.T. Jones, Y. Sugiura, S. Futaki, Cellular uptake of arginine-rich peptides: roles for macropinocytosis and actin rearrangement, Mol. Ther. 10 (2004) 1011-1022.

[38] I.A. Khalil, K. Kogure, S. Futaki. H. Harashima, High density of octaarginine stimulates macropinocytosis leading to efficient intracellular trafficking for gene expression, J. Biol. Chem. 281 (2006) 3544-3551.

[39] I.M. Kaplan, J.S. Wadia, S.F. Dowdy, Cationic TAT peptide transduction domain enters cells by macropinocytosis, J. Control. Release 102 (2005) 247-253.

[40] J.A. Swanson, C. Watts, Macropinocytosis, Trends. Cell. Biol. 5 (1995) 424-428.

[41] S. Falcone, E. Cocucci, P. Podini, T. Kirchhausen, E. Clementi, J. Meldolesi, Macropinocytosis: regulated coordination of endocytic and exocytic membrane traffic events, J. Cell Sci. 119 (2006) 4758-4769.

[42] S.R. Schwarze, A. Ho, A. Vocero-Akbani, S.F. Dowdy, In vivo protein transduction: delivery of a biologically active protein into the mouse, Science 285 (1999) 1569-1572.

[43] J.S. Wadia, S.F. Dowdy, Transmembrane delivery of protein and peptide drugs by TAT-mediated transduction in the treatment of cancer, Adv. Drug Deliv. Rev. 57 (2005)

579-596.

[44] A. Astriab-Fisher, D. Sergueev, M. Fisher, B.R. Shaw, R.L. Juliano, Conjugates of antisense oligonucleotides with the TAT and antennapedia cell-penetrating peptides: effects on cellular uptake, binding to target sequences, and biologic actions, Pharm. Res. 19 (2002) 744-754.

[45] M. Mie, F. Takahashi, H. Funabashi, Y. Yanagiba, M. Aizawa, E. Kobatake, Intracellular delivery of antibodies using TAT fusion protein A, Biochem. Biophys. Res. Commun. 310 (2003) 730-734.

[46] V.P. Torchilin, T.S. Levchenko, TAT-liposomes: a novel intracellular drug carrier, Curr. Protein Pept. Sci. 4 (2003) 133-140.

[47] V.P. Torchilin, R. Rammohan, V. Weissig, T.S. Levchenko, TAT peptide on the surface of liposomes affords their efficient intracellular delivery even at low temperature and in the presence of metabolic inhibitor, Proc. Natl. Acad. Sci. USA 98 (2001) 8786-8791.

[48] B. Gupta, T.S. Levchenko, V.P. Torchilin, Intracellular delivery of large molecules and small particles by cell-penetrating proteins and peptides, Adv. Drug Deliv. Rev. 57 (2005) 637-651.

[49] J.F. Liang, V.C. Yang, Insulin-cell penetrating peptide hybrids with improved intestinal absorption efficiency, Biochem. Biophys. Res. Commun. 335 (2005) 734-738.

[50] R. Trehin, H.P. Merkle, Chances and pitfalls of cell penetrating peptides for cellular drug delivery, Eur. J. Pharm. Biopharm. 58 (2004) 209-223.

[51] M. Zorko, U. Langel, Cell-penetrating peptides: mechanism and kinetics of cargo delivery, Adv. Drug. Deliv. Rev. 57 (2005) 529-545.

[52] K. Saar, M. Lindgren, M. Hansen, E. Eiriksdottir, Y. Jiang, K. Rosenthal-Aizman, M. Sassian, U. Langel, Cell-penetrating peptides: a comparative membrane toxicity study. Anal. Biochem. 345 (2005) 55-65.

[53] J.R. Pappenheimer, C.E. Dahl, M.L. Karnovsky, J.E. Maggio, Intestinal absorption and excretion of octapeptides composed of D amino acids, Proc. Natl. Acad. Sci. USA. 91 (1994) 1942-1945.

[54] H. Asada, T. Douen, Y. Mizokoshi, T. Fujita, M. Murakami, A. Yamamoto, S. Muranishi, Stability of acryl derivatives of insulin in the small intestine: relative importance of insulin association characteristics in aqueous solution, Pharm. Res. 11 (1994) 1115-1119.

[55] M. Morishita, A.M. Lowman, K. Takayama, T. Nagai, N.A. Peppas, Elucidation of the mechanism of incorporation of insulin in controlled release systems based on complexation polymers, J. Control. Release 81 (2002) 25-32.

[56] A. Elmquist, U. Langel, In vitro uptake and stability study of pVEC and its all-D analog, Biol. Chem. 384 (2003) 387-393.

[57] R. Tugyl, K. Uray, D. Ivan, E. Fellinger, A. Perkins, F. Hudecz, Partial D-amino acid substitution: Improved enzymatic stability and preserved Ab recognition of a MUC2 epitope

peptide, Proc. Nat. Acad. Sci. USA. 102 (2005) 413-418.

[58] R. Suzuki, Y. Yamada, H. Harashima, Efficient cytoplasmic protein delivery by means of a multifunctional envelope-type nano device, Biol. Pharm. Bull. 30 (2007) 758-762.

[59] B. Christiaens, J. Grooten, M. Reusens, A. Joliot, M. Goethals, J. Vandekerckhove, A. Prochiantz, M. Rosseneu, Membrane interaction and cellular internalization of penetratin peptides, Eur. J. Biochem. 271 (2004) 1187-1197.

[60] S. Violini, V. Sharma, J.L. Prior, M. Dyszlewski, D. Piwnica-Worms, Evidence for a plasma membrane-mediated permeability barrier to Tat basic domain in well-differentiated epithelial cells: Lack of correlation with heparan sulfate, Biochemistry. 41 (2002) 12652-12661.

[61] M.E. Lindgren, M.M. Hallbrink, A.M. Elmquist, U. Langel, Passage of cell-penetrating peptides across a human epithelial cell layer in vitro, Biochem. J. 377 (2004) 69-74.

[62] R. Trehin, U. Krauss, R. Muff, M. Meinecke, A.G. Beck-Sickinger, H.P. Merkle, Cellular internalization of human calcitonin derived peptides in MDCK monolayers: a comparative study with Tat(47-57) and penetratin(43-58), Pharm. Res. 21 (2004) 33-42.

[63] X. Zhang, L. Wan, S. Pooyan, Y. Su, C.R. Gardner, M.J. Leibowitz, S. Stein, P.J. Sinko, Quantitative assessment of the cell penetrating properties of RI-Tat-9: evidence for a cell type-specific barrier at the plasma membrane of epithelial cells, Mol. Pharm. 1 (2004) 145-155.

[64] A.M. Koch, F. Reynolds, H.P. Merkle, R. Weissleder, L. Josephson, Transport of surface-modified nanoparticles through cell monolayers, Chembiochem. 6 (2005) 337-345.

[65] D.J. Keljo, J.R. Hamilton, Quantitative determination of macromolecular transport rate across intestinal Peyer's patches, Am. J. Physiol. 244 (1983) G637-644.

[66] S.C. Silverstein, R.M. Steinman, Z.A. Cohn, Endocytosis, Annu. Rev. Biochem. 46 (1977) 669-722.

[67] S. Console, C. Marty, C. Garcia-Echeverria, R. Schwendener, K. Ballmer-Hofer, Antennapedia and HIV transactivator of transcription (TAT) "protein transduction domains" promote endocytosis of high molecular weight cargo upon binding to cell surface glycosaminoglycans, J. Biol. Chem. 278 (2003) 35109-35114.

[68] Y. Zheng, Y. Qiu, M.F. Lu, D. Hoffman, T.L. Reiland, Permeability and absorption of leuprolide from various intestinal regions in rabbits and rats, Int. J. Pharm. 185 (1999) 83-92.

[69] J. Guo, Q. Ping, G. Jiang, J. Dong, S. Qi, L. Feng, Z. Li, C. Li, Transport of leuprolide across rat intestine, rabbit intestine and Caco-2 cell monolayer, Int. J. Pharm. 278 (2004) 415-422.